

学位論文

The role of the SWI/SNF chromatin remodeling complex in maintaining
the stemness of glioma initiating cells

(グリオーマ幹細胞の幹細胞性維持に働く
クロマチン構造変換因子 SWI/SNF 複合体の解析)

平成 28 年 12 月博士（理学）申請

東京大学大学院理学系研究科

生物科学専攻 平松 寛明

Abstract

Glioma initiating cells (GICs) are thought to contribute to therapeutic resistance and tumor recurrence in glioblastoma, a lethal primary brain tumor in adults. Although the stem-like properties of GICs, such as self-renewal and tumorigenicity, are epigenetically regulated, the role of a major chromatin remodeling complex in human, the SWI/SNF complex, remains unknown in these cells. Here, I demonstrate that the SWI/SNF core complex, which is associated with a unique corepressor complex through the d4-family proteins, DPF1 or DPF3a, plays essential roles in stemness maintenance in GICs. The serum-induced differentiation of GICs downregulated the endogenous expression of *DPF1* and *DPF3a*, and the shRNA-mediated knockdown of each gene reduced both sphere-forming ability and tumor-forming activity in a mouse xenograft model. Rescue experiments revealed that DPF1 has dominant effects over DPF3a. Notably, whereas we have previously reported that d4-family members can function as adaptor proteins between the SWI/SNF complex and NF- κ B dimers, this does not significantly contribute to maintaining the stemness properties of GICs. Instead, these proteins were found to link a corepressor complex containing the nuclear receptor, TLX, and LSD1/RCOR2 with the SWI/SNF core complex. Collectively, these results indicate that DPF1 and DPF3a are potential therapeutic targets for glioblastoma.

Table of Contents

Introduction.....	p.4
Results.....	p.9
Discussion.....	p.20
Materials and Methods.....	p.24
Acknowledgements.....	p.31
References.....	p.32
Figures and Tables.....	p.38

Introduction

Glioblastoma multiforme (GBM) and glioma initiating cells (GICs)

Glioblastoma multiforme (GBM) is the most common malignant brain tumor in adults and remains incurable with an average survival of slightly more than 1 year past the initial diagnosis in spite of modern surgical and medical therapies.

Tumors are comprised of a highly heterogeneous population of cells and contain a subset of stem-like cells called cancer stem cells (CSCs), which have the ability to self-renew, differentiate into various cell types and regenerate tumors. Similar to other malignant tumors, large body of evidence now indicates that stem-like cells, designated as glioma initiating cells (GICs), are thought to drive GBM propagation and cause therapeutic resistance in these tumors [1-3, 6].

Stemness properties of GICs are characterized by their capacity for self-renewal as well as differentiation, expression of some neural stem/progenitor cell markers and their ability to induce tumorigenesis in immunocompromised mice with a very small number of cells [4-6]. To demonstrate the self-renewal and differentiation of single cancer stem cells, it will be important to show that single cells from a prospectively identified population of cancer stem cells can self-renew to generate phenotypically similar tumorigenic daughter cells, as well as differentiate into phenotypically diverse non-tumorigenic daughter cells during tumorigenesis in vivo [5]. However, it is possible that tumorigenesis by single cancer stem

cells is inherently inefficient because microenvironments that are permissive for tumorigenesis could be rare under many circumstances [1, 4-6].

GICs have been reported previously to retain their stemness properties when cultured as non-adherent spheres in a defined medium without serum supplemented with EGF and bFGF even more than 70 passages so far [7]. Orthotopic xenotransplantation of as few as 50 GICs leads to formation of tumors in the brains of SCID mice [8]. On the other hand, the differentiation of GICs can be induced by culturing the cells as an adherent monolayer in medium containing serum [7]. During the differentiation, GICs lose their stemness properties like potent tumorigenesis and stem cell marker genes expression, and orthotopic xenotransplantation of as many as 10^5 differentiated cells fails to initiate tumors in the brains of any SCID mice [7, 8].

Three independent cell isolates from GBM patients (TGS-01, -04 and -05) have been reported previously to have these GIC properties when cultured as non-adherent spheres in a defined medium without serum [9]. These cells have the ability to self-renew and mimic the original tumor after transplantation into the brains of immunocompromised mice [9]. The differentiation of these three GIC isolates can be induced by culturing the cells as an adherent monolayer in medium containing serum [7, 9].

Epigenetics of GICs

Chromatin structure modification has been shown to be an important determinant of GIC stemness maintenance as well as the induction of their

differentiation [10, 11]. Recently, using gene expression data from both stem-like and differentiated cell populations, it was shown that the simultaneous expression of four core transcription factors, POU3F2, SALL2, SOX2, and OLIG2, can reprogram differentiated GBM cells into spherogenic stem-like tumor-propagating cells [8]. These results demonstrate a plastic developmental hierarchy in GBM cell populations and reveal essential roles of epigenetic regulation in these biological processes [12].

Function and components of SWI/SNF complex

In humans, the ATP-dependent chromatin remodeling factor, SWI/SNF complex, has been reported to play essential epigenetic roles in many biological processes [13-15]. As the catalytic subunit, each SWI/SNF complex has a single molecule of either BRG1 or Brm, but not both (Fig. 1). The molecular components of these SWI/SNF complexes are now known to be highly polymorphic, in which some subunits that are encoded by homologous gene family members are integrated into the specific position of the complex in a mutually exclusive manner [13, 14, 16]. Importantly, exchange of a subunit with another family member has often been observed during several developmental processes within either the SWI/SNF core complex or its strongly associated cofactor proteins. Some of those exchanges are anticipated to be crucial for these developmental transitions. For example, BRG1 is much more abundant than Brm in embryonic and neural stem cells and is thus thought to be the major

functional catalytic subunit in these cellular contexts [13, 14, 17-19]. In a similar mutually exclusive manner, one of DPF1, DPF2 (REQ/BAF45D), DPF3a or DPF3b (a splicing variant of DPF3a), which comprise the d4-family proteins, is a cofactor that substoichiometrically interacts with human SWI/SNF complexes.

d4-family proteins

We have previously demonstrated that DPF2 functions as an efficient adaptor protein between the SWI/SNF complex and the RelB/p52 dimer [20]. By examining all of the d4-family proteins (DPF1, 2, 3a and 3b), we further found that high level exogenous expression of each of these factors can potentiate the transactivating activity of typical NF- κ B dimers including RelA/p50, which is responsible for the canonical NF- κ B pathway, and RelB/p52, which is the most downstream factor of the non-canonical NF- κ B pathway [21]. In addition, we demonstrated from our analysis in 293FT cells that DPF3a and 3b are the most effective cofactors of the SWI/SNF complex for RelA/p50 activation. These previous observations are schematically represented in Figure 2.

The propose of this study

In the current study, I show that knockdown of either *DPF1* or *DPF3a* promptly abolishes stemness maintenance of GICs. I have demonstrated that through these d4-family proteins, a distinct SWI/SNF core complex is associated with specific corepressor complexes and further that such larger

SWI/SNF complex is an essential determinant of the key features of GICs. Therefore, DPF1 and DPF3a would be possible new therapeutic targets for GBM.

Results

***DPF1* and *DPF3a/b* transcripts are abundant in GICs in sphere cultures but are downregulated upon differentiation.**

To identify the genes enriched in GIC sphere cultures, I isolated total RNA and protein from 3 respective pairs of sphere and differentiated monolayer GIC cultures (TGS-01, -04 and -05 [9]). By qRT-PCR and western blotting using these GIC preparations, I checked the expression of the POU3F2, SOX2, SALL2 and OLIG2, which have been reported to be required for the reconstitution and maintenance of stemness [8] (Fig. 3, 4, 5). By comparing the RNA and protein levels between the sphere and differentiated monolayer GIC cultures, I found that all 4 transcription factors were at higher levels in sphere culture, indicating that these GIC cultures had very similar properties to stem-like tumor propagating cells (TPCs) reported previously [8].

Using the same samples, I next examined the expression levels of core components of SWI/SNF complex and of several proteins reported to be strongly associated with SWI/SNF complex. The mRNA (Fig. 3, 5) and protein (Fig. 6) levels of BRG1, the catalytic subunit thought to be involved in the stemness maintenance in embryonic and neuronal stem cells, were higher in sphere cultures than in differentiated cultures of all three GICs. Interestingly, among the d4-family members, *DPF1* and *DPF3a/b* were found to be more abundant in sphere cultures (Fig. 3), although the expression levels of *DPF3a/b* varied among the three GIC

sphere cultures (Fig. 5).

DPF1 and DPF3a play important roles in maintaining GIC stemness

To test the possible involvement of BRG1 and the d4-family proteins in stem cell maintenance in GICs, I performed respective knockdown experiments using at least two sets of short-hairpin (sh)RNAs with efficient suppressing activity. shRNAs used in this study were either previously reported [21] or newly prepared (Fig. 7) and they were selected by the following criteria: mRNA levels of each target were specifically reduced to 40% in 293FT or MDA-MB-231 cells. Preliminary experiments indicated that the biological effects of a *DPF1* and *DPF3a* knockdown seemed to be so rapid that I could not isolate stable transductants in non-adherent sphere culture by puromycin selection. I therefore employed shRNA expression lentivirus vectors coexpressing GFP. To evaluate the stemness of GICs, I performed sphere forming assays in which GFP positive cells were single-sorted into a well at 48 hours after transduction and sphere forming activity was evaluated. The sphere forming assay is a widely used to demonstrate the self-renewing ability and believed to be able to evaluate the potential of a cell to behave as a stem-like cell when removed from its in vivo niche [22]. The knockdown of *BRG1*, *DPF1*, *DPF3a*, and *DPF3b* drastically reduced the sphere forming activity of TGS-01, whereas a *DPF2* knockdown showed only marginal effects in this assay (Fig. 8). To test whether this important function of DPF1 and DPF3a could be extended to the other GICs, I subjected TGS-04 and TGS-05 cells to a *DPF1* or *DPF3a*

knockdown and found that, similar to TGS-01, sphere forming activity was reduced in both instances (Fig. 9).

To eliminate the possibility of off-target effects by the shRNA constructs, rescue experiments were performed. Since the loss of stemness can be detected very early after vector transduction, I designed and developed dual lentivirus expression vectors (Fig. 10) carrying expression units of both shRNAs (driven by the *mU6* pol III promoter) and the corresponding cDNA (driven by the *EF1 α* pol II promoter known to be relatively resistant to gene silencing in stem cells), where the cDNAs were designed to be resistant to the corresponding shRNA. In the case of *BRG1*, *DPF1* and *DPF3a*, the simultaneous expression of corresponding cDNA partially rescued the sphere forming activity (Fig. 11). Interestingly, *DPF3a* knockdown was also rescued by *DPF1* cDNA expression, whereas *DPF1* knockdown was not significantly rescued by the exogenous expression of *DPF3a* (Fig. 11). These results suggest that *DPF1* has dominant effects over *DPF3a* in terms of stem cell maintenance. Because rescue experiments using *DPF3b* cDNA in *DPF3b* knockdown cells were not successful and also because the mRNA levels of *DPF3b* are close to the limit of detection by qRT-PCR in these GICs, I did not further analyze *DPF3b*. It was notable that the exogenous expression of FLAG-tagged d4-family proteins, *BRG1* and *Brm* in TGS-01 cells did not increase sphere forming activity (Fig. 12), indicating that the endogenous levels of these proteins were at saturated levels sufficient to maintain stemness.

The extent of rescues using dual expression vectors were only partial.

These results might reflect the prompt effects of shRNAs which appeared before the exogenous protein expression reached stable levels. To exclude this possibility, I prepared TGS-01 cells stably expressing the each d4-family proteins in advance and additionally transduced with shRNA expression vectors. The expression levels of exogenous DPF1 and DPF3a proteins were roughly the same, whereas the expression level of DPF2 was slightly lower (Fig. 13). As shown in Figure 14, when shDPF1 and shDPF3a were introduced into cells expressing the corresponding cDNA, the sphere forming activity was partially recovered again. Moreover, DPF1-introduced cells showed higher sphere forming activity compared with EV-2-introduced cells did when shDPF3a was expressed by another virus vector. On the other hand, cells exogenously expressing DPF3a were found to be sensitive to an additional *DPF1* knockdown. These results confirmed the previous observations with dual expression vectors, i.e. that DPF1 is dominant over DPF3a. In these experiments however, the recovery of sphere forming activity through corresponding cDNA expression was generally incomplete. Whereas the *EF1 α* promoter used to express d4-family proteins has been reported to be active in most cell types including primary and stem cells, and to be relatively resistant to gene silencing, it is now known that its activity is gradually lost during long-term culture in embryonic stem cells, neural precursors and neuronal cells [23, 24]. These results showing insufficient rescues in GICs might be at least partly derived from the difficulty in long-term exogenous expression in GICs.

BRG1 can be functionally substituted by Brm as a catalytic subunit of the SWI/SNF core complex that contributes to GIC stemness.

Whereas the higher expression levels of *Brm* mRNA in differentiated cultures were basically similar among the three GICs cultures, *Brm* mRNA levels in sphere cultures of TGS-04 and TGS-05 were considerably higher than in the TGS-01 cultures (Fig. 5). When Brm proteins in TGS-04 and TGS-05 cells were analyzed by western blotting (Fig. 6), unlike mRNA levels, the protein levels were higher in sphere cultures than in differentiated cultures, indicating that there would be some post-transcriptional regulation of Brm expression in these cells. These results also suggest heterogeneity in the SWI/SNF components among the three GIC cultures.

I further found that the sphere forming activity of both TGS-04 and TGS-05 was insensitive to both *BRG1* and *Brm* knockdown (Fig. 15a, b). This finding contrasted with the observations in TGS-01 cells (Fig. 8), in which the *BRG1* knockdown caused a reduction in sphere forming activity. I hypothesized that because of the high expression of both BRG1 and Brm proteins in TGS-04 and 05 cells (Fig. 6), a single knockdown of either may not have significantly affected sphere forming activity. This was probably because Brm can also function as an effective catalytic subunit of SWI/SNF complex for the stem cell maintenance of GICs.

To test whether Brm could indeed functionally substitute for BRG1, I next coexpressed Brm and shBRG1 in TGS-01 cells. The sphere forming

activity in these transfectants was rescued by Brm expression (Fig. 16), whereas the exogenous expression of Brm was not substantially affected the sphere forming activity (Fig. 12). These results indicate that Brm, if expressed in GICs at high protein levels, can also contribute to the maintenance of stemness. Therefore, at least in terms of maintaining GIC stemness, the frequently observed enrichment of BRG1 in sphere cultures does not mean that Brm cannot also perform the same biological activity.

***DPF1* and *DPF3a* knockdowns in GICs produce strong anti-tumorigenic activity.**

It is reported that, when GICs are injected into the brain of immunocompromised mice, these mice were gradually lose weights with neurological symptoms including lethargy, poor feeding, paralysis, appearance of distress such as poor mobility, self-mutilization, hunched posture, dehydration and skin ulcers, and eventually die due to the tumor progression with infiltration into the surrounding normal brain [25]. To further confirm the stemness maintenance function of DPF1 and DPF3a, I examined the tumorigenicity which is the representative stemness property. TGS-01 cells transduced with shDPF1 or shDPF3a expression vectors as well as an EV-2 (control) cells were orthotopically inoculated into immunocompromised mice (nude mice). Although I saw a rapid reduction in the survival rate of mice inoculated with the control cells, both shDPF1 and shDPF3a expression improved this survival rate (Fig. 17). All mice, the body weights of which was measured during 1-4 days before death (7

mice) had lost their body weight compared with the previous time point of measurement (Fig. 18) In these mice, I often observed neurological symptoms such as poor mobility. Furthermore, when some dead mice were dissected, the invasion of the tumor in their brain was always observed. Notably, the expression of shDPF1 produced much greater effects compared with shDPF3a (5/6 mice showed full survival). These results confirmed that DPF1 has more profound effects on the maintenance of GIC stemness and thus further revealed that it has potential as a therapeutic target in GBM.

Stemness maintenance by DPF1 and DPF3a does not require NF- κ B activation

In our previous studies using epithelial tumor cell lines, the d4-family members were shown to function as adaptor proteins linking the SWI/SNF complex with NF- κ B dimers [20, 21]. Considering the strong dependency of GIC stemness maintenance on BRG1, DPF1 and DPF3a expression, I next tested whether SWI/SNF-dependent NF- κ B activation contributed to this biological activity. I κ B α is a NF- κ B inhibitor, and I κ B α SR is its mutant, which cannot be phosphorylated at the specific serine residues targeted by IKK and therefore reduces NF- κ B activity efficiently [26]. When I κ B α SR was introduced into TGS-01 cells, we did not detect any effects on sphere forming activity; the percentages of sphere forming cells in EV-2 transduced cells and I κ B α SR expressing cells were 20.57 ± 1.59 % and 21.35 ± 0.60 % respectively. To examine the activation status of

endogenous NF- κ B in GICs, we performed immunofluorescence assays and investigated the subcellular localization of NF- κ B dimers. As a result, I found that both RelA and RelB were predominantly localized to the cytoplasm in TGS-01 cells (Fig. 19). Furthermore, the expression levels of *IL6* and *IL8*, which are representative SWI/SNF-dependent NF- κ B target genes, were very low in sphere cultures compared to those in differentiated cultures (Fig. 20). Collectively, these results suggest that DPF1 and DPF3a have distinct functions other than adaptors between NF- κ B and the SWI/SNF complex in GICs to play essential roles in the maintenance of stemness.

Formation of a large complex comprising the SWI/SNF core complex and a corepressor complex requires DPF1 and DPF3a adaptors.

Given the observation of the prompt and strong suppression of stemness maintenance by shDPF1, and to a lesser extent by shDPF3a, I hypothesized that DPF1 as well as DPF3a can function as adaptors between SWI/SNF core complex and key transcriptional regulators which are essential for stemness of GICs. To examine this possibility, antibodies against several candidate proteins were tested whether they are able to coimmunoprecipitate with subunits of the SWI/SNF complex. Among the possible candidates that would form large complexes with SWI/SNF core complex, I found that antibodies against TLX (NR2E1), LSD1 (lysine-specific demethylase 1) and RCOR2 (REST corepressor 2; CoREST2) coimmunoprecipitate both BRG1 and BAF155 from TGS-01

cell lysates (Fig. 21a, b). TLX, a nuclear orphan receptor with transcriptional suppressing function, has been previously shown to control the neuronal stem cells [27-29] and to be essential for maintaining the stemness of GICs by knockdown experiments [30]. LSD1, a negative epigenetic regulator with histone demethylase activity, has also been reported to regulate GIC stemness in combination with RCOR2 (REST corepressor2; CoREST2), a well-known corepressor [8]. Importantly, the protein levels of TLX was unchanged after induction of differentiation of these three GIC cultures whereas those of LSD1 and RCOR2 were enriched in sphere cultures (Fig. 6). When TGS-01 lysates were immunoprecipitated using a TLX antibody, I detected LSD1 and HDAC2 in these immunoprecipitates (Fig. 21a). Moreover, when these lysates were immunoprecipitated with an LSD1 antibody, I detected RCOR2, and *vice versa* (Fig. 21b), confirming previous reports of tight dimer formation between these two proteins [8, 31]. Similarly, when TGS-04 and TGS-05 cellular lysates were immunoprecipitated with TLX antibody, both BRG1 and BAF155 were detected in the immunoprecipitates (Fig. 22). Furthermore when lysates of TGS-01 cells exogenously expressing FLAG-tagged DPF1 or DPF3a were immunoprecipitated with either a TLX or LSD1 antibody, DPF1 or DPF3a as well as BRG1, BAF155 and LSD1 were detected (Fig. 23a, b). FLAG-tagged DPF2 was also detected but at considerably lower levels. Overall, these results suggest that DPF1 and DPF3a can function as adaptor proteins linking the SWI/SNF complex and corepressor complexes containing TLX and LSD1/RCOR2.

Considering that the biochemical protocols used to lyse cells and isolate protein complexes from extracts are prone to disrupt *bona fide* protein interactions in cellular nuclei, I next used the *in situ* proximity ligation assay (PLA) as this method is suitable for visualizing interactions between proximally positioned proteins in cells after fixation of large labile complexes. A schematic diagram of this method is shown in Figure 24. In the preliminary studies using normal IgG, only marginal signals were detected. All of the proteins analyzed (BRG1, BAF155, TLX and LSD1) were confirmed to be strictly localized in the nucleus by immunofluorescence assay (Fig. 25) and the same antibodies were used for PLA. Similar to the positive control using the anti-BRG1/anti-BAF155 antibody pair (two subunits of SWI/SNF core complex), the anti-BRG1/anti-TLX, anti-BRG1/anti-LSD1, anti-LSD1/anti-TLX, and anti-LSD1/anti-BAF155 antibody pairs detected close localization between these 5 pairs of proteins (Fig. 26). When each single antibody was used, there were only a few signals detected (Fig. 26). TGS-01 cells transduced with FLAG-tagged DPF1 expression vector were analyzed by PLA, I was able to detect close localization between DPF1 and TLX, DPF1 and LSD1, and DPF1 and BAF155 (Fig. 27), whereas when only anti-FLAG antibody was used, there was only a few signals. From these results, the corepressor complex including TLX and LSD1 were shown to be closely associated with the SWI/SNF core complex. To examine impacts of *DPF1* knockdown on this larger SWI/SNF complex, TGS-01 cells expressing shDPF1 were analyzed by PLA. The results indicated that signals detecting

the proximal localization of BRG1 and TLX or BRG1 and LSD1 were drastically decreased, whereas those for BRG1 and BAF155 or LSD1 and TLX were unaffected (Fig. 28). These observations are consistent with the idea that DPF1 connects the SWI/SNF core complex and corepressor complex containing TLX and LSD1/RCOR2.

Discussion

I have here described differences in the subunit composition of the SWI/SNF core complex and their associated cofactors between sphere and differentiated monolayer cultures of GICs. I have also shown that among the mRNAs enriched in GIC sphere cultures, DPF1 and DPF3a play key roles in the stemness maintenance of these cells. By shRNA-mediated knockdowns in GICs, both proteins were shown to be essential for growth and sphere formation in culture and tumor propagation in a mouse orthotopic transplantation model (Fig. 8, 9, 11, 14, 17). The effects of *DPF1* or *DPF3a* knockdowns on cellular survival and sphere formation were very rapid, which in itself suggests that DPF1 and DPF3a could be direct therapeutic targets for the suppression of GICs. When TGS-01 cells were transduced with vectors expressing shDPF1 or shDPF3a and transplanted into nude mice, the shDPF1 expressing cells showed much stronger anti-tumor forming activity than those transduced with shDPF3a (Fig. 17). This result is consistent with the findings from the *in vitro* sphere forming assays indicating that a *DPF1* knockdown cannot be significantly rescued by DPF3a cDNA expression, whereas the sphere forming activity of *DPF3a*-knockdown cells can be rescued by DPF1 cDNA expression (Fig. 11, 14). Overall, DPF1 shows potential as a future therapeutic target for GBM.

Coimmunoprecipitation experiments revealed the presence of a large protein complex containing both SWI/SNF core complex and a corepressor

complex (Fig. 21, 22, 23). However, a detailed description of this complex was difficult probably because the large complex is fragile. An antibody to the putative component could partly disrupt this complex when it binds to its antigen. It is also possible that the formation and dissociation of this large complex are in equilibrium in a cell. To resolve this problem, I fixed the labile large complexes in cells, and monitored proximally positioned proteins using PLAs (Fig. 26, 27). By this method, I was able to detect a close association between the SWI/SNF core complex and corepressor complex in the nuclei of GICs. The corepressor complex was found to be composed of the nuclear receptor TLX and LSD1/RCOR2 using various different pairs of antibodies. Since TLX is the only transcription factor which can bind directly to DNA in this large complex, I believe that this large complex has a transcriptional suppression function mediated through TLX in a SWI/SNF-dependent manner. In this regard, it is worth noticing that the well-known target genes that are suppressed by TLX, *P21* [32, 33] and *BMP4* [34], were found to be upregulated upon the induction of GIC differentiation (Fig. 29). Considering that the suppression of these two genes have been reported to be essential for stemness maintenance of GICs [35, 36], they might be the direct targets of the large complex. The model of the large complex formation is schematically represented in Figure 30. From these observations, I believe that TLX plays a crucial function in this large protein complex to maintain GICs.

It is noteworthy that we have previously observed large complex formation between the SWI/SNF core complex and a complex containing

NRSF/COREST/mSin3A in epithelial tumors [37]. A subset of the SWI/SNF core was present in this larger complex and was found to be responsible for the suppression of such neuronal genes as *synaptophysin*, *SCGI* and *synapsin1* in non-neural cells. The representative SWI/SNF core complex is also present and contributes to the basal expression of the *IL-6* gene in the same cell.

Shortly after the knockdown of *DPF1*, the stem-cell like properties of the GICs were rapidly suppressed and the proximal locations between BRG1 and TLX or between BRG1 and LSD1 were disrupted, whereas those between BRG1 and BAF155 or between TLX and LSD1 were unaffected (Fig. 28). Although the exact molecular components of the entire complex remain to be resolved, in the large complex detected in these current analyses, DPF1 probably function as linkers between the SWI/SNF core and corepressor.

It should be pointed out in this regard also that a previous search was conducted for candidates for direct regulatory targets (transcription factors and epigenetic regulators) of the four core transcription factors (POU3F2, SOX2, SALL2 and OLIG2) that would mediate stemness maintenance by analyzing core nodes in the transcriptional network controlled by these four core factors [8]. Intriguingly, DPF1 was among those candidates and is suggested to function downstream of OLIG2. Interestingly, some other components in larger SWI/SNF complexes were identified, LSD1 and RCOR2 were also included in the list of candidates. Therefore, I believe that I have here isolated a protein complex that assembles many key

regulators to directly epigenetically regulate stemness in GICs. The possible adaptor protein, DPF1, which links the core SWI/SNF and corepressor complexes, is likely to be a very promising therapeutic target for disrupting only the large complex in GICs.

Materials and Methods

Cell culture

Three independent glioma initiating cells (GICs) termed TGS-01, TGS-04 and TGS-05 were established as described previously [9]. All human materials and protocols used in this study were approved by the ethics committee of the University of Tokyo Hospital (24-69-250809) and Medical Mycology Research Center (MMRC), Chiba University (#10). All methods were performed in accordance with each university's guideline and regulation. Informed consent was obtained from all patients. GICs were passaged in DMEM/F12 serum-free medium (Thermo Fisher Scientific) supplemented with B27 (Thermo Fisher Scientific), 20 ng/ml of EGF, and 20 ng/ml of bFGF (both from PeproTech) using ultra-low attachment dishes or flasks. Dulbecco's modified Eagle's medium containing 10% fetal bovine serum (FBS) was used to induce the differentiation of GICs and to passage 293FT and PLAT-A human embryonic kidney cells in culture.

Plasmid construction

For lentivirus construction, the DNA fragment containing *EF1 α* promoter region was amplified by PCR from pXL001 (26122 [38], Addgene) using the primer sets listed in Table 1 and digested with NheI. pLSP [39] was digested with ClaI, blunt ended using T4 DNA Polymerase and then digested with XbaI. The resulting 1.5 kb and 5.1 kb fragments were ligated to generate pLE. Pairs of oligonucleotides containing multi cloning sites

(MCS) were synthesized as listed in Supplemental Table S1 and inserted into the EcoRV/ClaI sites of pLE to generate pLE-MCS. IRES-EGFP and IRES-Puro^r fragments were obtained by PCR from pMXs-IG [40] and pMXs-IP [40], respectively, using primer sets listed in Table 1 and were digested with XbaI and ClaI. The resulting 1.3kb and 1.2 kb fragments were inserted into the XbaI/ClaI site of pLE-MCS to generate pLE-IG (EV-2) and pLE-IP (EV-3), respectively.

For shRNA expression vectors, pairs of oligonucleotides encoding gene-specific short hairpin RNA (shRNA) were synthesized as listed in Table 1 and inserted into the BbsI/EcoRI sites of pmU6 [41]. The pmU6 derivatives shCre#4 [42], shBrm#4 [43] shDPF1-CDS#1 [21] and shDPF3a-3'UTR#2 [21] were previously described. These pmU6-based plasmids were doubly digested with BamHI and EcoRI, and inserted into the same sites of pSSCG [39] (EV-1) or pLE-IG (EV-2).

For exogenous expression, pairs of oligonucleotides encoding a 3×FLAG tag were synthesized as listed in Table 1, annealed, extended, digested with BglII and MfeI, and inserted into the BglII/MfeI site in MCS of pLE-IG and pLE-IP. DPF1, DPF2, DPF3a, DPF3b, BRG1 and Brm fragments were amplified by PCR using primer sets listed in Table 1 and cloned into the BamHI-EcoRI site of pCR2.1. DPF1, DPF2, DPF3a and DPF3b fragments were digested with EcoRI and SalII, and inserted into the MfeI/XhoI site in MCS of pLE-IG and pLE-IP. BRG1 fragment was digested with MfeI and XbaI, and inserted into the MfeI/XbaI site in MCS of pLE-IG and pLE-IP. Brm fragment was digested with EcoRI and XhoI,

and inserted into the EcoRI/XhoI site in MCS of pLE-IG and pLE-IP. Site-directed mutagenesis was performed using a KOD-Plus-Mutagenesis kit (TOYOBO) in accordance with the manufacturer's instructions to generate BRG1 shRNA resistant mutant with primer sets listed in Table 1. IκBαSR expression vector was kindly gifted by Prof. Shoji Yamaoka [26]. All plasmids were confirmed by DNA sequencing.

DNA transfection and retro/lentivirus preparation

For the transfection of plasmids into cells, Lipofectamine 2000 (Thermo Fisher Scientific) was used in accordance with the manufacturer's instructions. Vesicular stomatitis virus-G (VSV-G) pseudotyped retrovirus vectors were produced using the prepackaging cell line PLAT-A. VSV-G pseudotyped lentivirus vectors were produced with the prepackaging cell line 293FT, using the ViraPower Lentiviral Expression System (Thermo Fisher Scientific), in accordance with the manufacturer's instructions. Three hours after transfection, the medium was changed to virus production serum-free medium (VP-SFM; Thermo Fisher Scientific) containing 4 mM L-glutamine. The transfection supernatant was collected after 24 and 48 hours after transfection, filtered through a 0.45-μm filter, and centrifuged at $6000 \times g$ at 4°C for 16 hours. The pellets were suspended in culture medium for GICs. For transduction, GICs were incubated with the virus vector stocks at 37°C for 4 hours. All experiments were performed at low MOI (< 0.3).

RNA preparation and quantitative RT-PCR

Total RNA was extracted using a mirVana microRNA Isolation Kit (Thermo Fisher Scientific). All RNA samples were then treated with TURBO DNase enzyme (TURBO DNA-free Kit; Thermo Fisher Scientific). To detect mRNAs, cDNA was synthesized with a PrimeScript RT Master Mix (TaKaRa Bio) in accordance with the manufacturer's instructions. Quantitative real-time RT-PCR (qRT-PCR) was performed using a SYBR Select Master Mix (Thermo Fisher Scientific). *GAPDH* mRNA was used as an internal control. The primer pairs used are listed in Table 2. qRT-PCRs were performed in triplicate using a StepOne Plus real-time PCR system (Thermo Fisher Scientific).

Western blotting

Total protein extracts were prepared by boiling the cells in 2×SDS sample buffer for 10 min at 95°C. The proteins were then resolved by 10% SDS-PAGE and transferred onto Immobilon-P PVDF membranes (Millipore). Western blotting was performed by incubating the membrane in Can Get Signal Solution I (TOYOBO) containing primary antibodies overnight at 4°C. After three washes with Tris-buffered saline (TBS) containing 0.1% Tween 20, the membranes were incubated in Can Get Signal Solution II (TOYOBO) containing secondary antibodies [donkey anti-rabbit-horseradish peroxidase (AP182P; Millipore), Peroxidase AffiniPure Donkey Anti-Mouse IgG (715-035-150; Jackson immunoresearch), Peroxidase AffiniPure Donkey Anti-Goat IgG

(705-035-147; Jackson immunoresearch) and Anti-DDDDK-tag mAb-HRP-DirecT (M185-7; MBL)] for 1 hour at room temperature (RT). Signals were detected on an AE-9300H-CP Ez-CaptureMG (ATTO) imaging analyzer using ECL Western Blotting Substrate (Promega) or Immunostar DL (WAKO). The primary antibodies used are listed in Table 3.

Single-cell sphere formation assay

Two days after the transduction with shRNA expression retrovirus vectors (pSSCG) or shRNA/cDNA dual expression lentivirus vectors (pLE-IG), GICs were dissociated with TrypLE express (Thermo Fisher Scientific) and GFP (+)/7-AAD (-) cells were sorted by FACS ARIA I or ARIA II (Becton Dickinson) at a density of 1 cell per well into ultra-low attachment 96-well plates (Corning) in 100 μ l of DMEM/F12 serum-free medium. After 2 weeks, the percentage of wells containing spheres was calculated.

Intracranial proliferation assay

Two days after transduction with shRNA expression lentivirus vectors (pLE-IG), GICs were dissociated and GFP (+)/7-AAD (-) cells were sorted by FACS ARIA I, centrifuged and resuspended in DMEM/F12 serum-free medium. A total of 3×10^3 cells (2 μ l) were injected stereotactically into the right cerebral hemisphere of 6-week-old female BALB/c nu/nu mice (CLEA Japan) at a depth of 3 mm. All animal experimental protocols were performed in accordance with the policies of the Animal Ethics Committee

of the University of Tokyo and performed in compliance with University's Guidelines for the Care and Use of Laboratory Animals.

Immunoprecipitation

Cells were lysed with a buffer containing 50 mM Tris-HCl (pH 7.5), 140 mM NaCl, 1 mM MgCl₂, 0.5mM DTT, 0.1% Tween20, protease inhibitor cocktail (Nacalai Tesque) and phosphatase inhibitor cocktail (Nacalai Tesque). Immunoprecipitation were performed using Dynabeads Protein G (Thermo Fisher Scientific) in accordance with the manufacturer's instructions. The antibodies used are listed in Table 3.

Immunofluorescence and proximity ligation assay

For immunofluorescence, GICs were seeded onto an 8-Well Lab-Tek II chamber slide (Nunc) coated with poly-L-lysine and left 5 minutes. The cells were then fixed with PBS containing 4% paraformaldehyde (Nacalai Tesque) for 10 min at room temperature (RT), washed twice with PBS and permeabilized with 0.2% Triton X-100 PBS for 15 min at RT. After washing twice with PBS, blocking was performed using a 1:1 mixture of 5% BSA, 0.02% NaN₃ PBS and Blocking one (Nacalai Tesque) for 1 hour at 37°C. The samples were then incubated overnight at 4°C with primary antibodies (listed in Table 3) in blocking buffer. The samples were washed twice and subsequently incubated with Alexa Fluor 546 or 488 conjugated secondary antibodies (Thermo Fisher Scientific, 1:1000) in blocking buffer in the dark for 1 hour at RT. The samples were mounted in Vectashield

Mounting Medium with DAPI (Vector Laboratories). Fluorescence was detected using a fluorescence microscope (BZ-X710; Keyence). Images were processed using Adobe Photoshop CS3 software.

For the proximity ligation assay (PLA), GICs were seeded, treated and incubated with primary antibodies as described above. The PLA was performed using the Duolink In Situ Starter Set ORANGE (Sigma) in accordance with the manufacturer's instructions. Anti-mouse MINUS and anti-rabbit PLUS PLA probes were used. Fluorescence was detected using a fluorescence microscope (BZ-X710; Keyence).

Statistical analysis.

Results are presented as means \pm S.D. Statistical significance for qRT-PCR assays and single-cell sphere formation assay was determined using a two-tailed Student's t-test. For the survival analysis shown in Figure 13, differences in survival rates were evaluated by the log-rank test.

Acknowledgements

I'm very grateful to my supervisor, Prof. Kensuke Miyake (Division of Infectious Genetics, Institute of Medical Science, the University of Tokyo) for his great and kind help during my doctoral course.

I would like to express the deepest appreciation to Professor Hideo Iba (Division of Host-Parasite Interaction, Institute of Medical Science, the University of Tokyo: Division of RNA Therapy, Medical Mycology Research Center, Chiba University) for his guidance during my doctoral course. And I thank all the members in our laboratory for their advice. Especially, I appreciate Kazuyoshi Kobayashi, Kyousuke Kobayashi, and Takeshi Haraguchi, who are the members in our laboratory for their help laboratory experiments.

I would like to express great thanks to Prof. Tomoki Todo and Dr. Yasushi Ino (Division of Innovative Cancer Therapy, and Department of Surgical Neuro-Oncology, Institute of Medical Science, the University of Tokyo) for their help on culture of GICs and mouse xenograft assay.

I would like to thank Prof. Shoji Yamaoka (Department of Molecular Virology, Tokyo Medical and Dental University) for his kind support.

References

1. Singh, S.K., et al., *Identification of human brain tumour initiating cells*. Nature, 2004. **432**(7015): p. 396-401.
2. Bao, S., et al., *Glioma stem cells promote radioresistance by preferential activation of the DNA damage response*. Nature, 2006. **444**(7120): p. 756-60.
3. Chen, J., et al., *A restricted cell population propagates glioblastoma growth after chemotherapy*. Nature, 2012. **488**(7412): p. 522-6.
4. Reya, T., et al., *Stem cells, cancer, and cancer stem cells*. Nature, 2001. **414**(6859): p. 105-11.
5. Pardal, R., M.F. Clarke, and S.J. Morrison, *Applying the principles of stem-cell biology to cancer*. Nat Rev Cancer, 2003. **3**(12): p. 895-902.
6. Singh, S.K., et al., *Identification of a cancer stem cell in human brain tumors*. Cancer Res, 2003. **63**(18): p. 5821-8.
7. Lee, J., et al., *Tumor stem cells derived from glioblastomas cultured in bFGF and EGF more closely mirror the phenotype and genotype of primary tumors than do serum-cultured cell lines*. Cancer Cell, 2006. **9**(5): p. 391-403.
8. Suvà, M.L., et al., *Reconstructing and reprogramming the tumor-propagating potential of glioblastoma stem-like cells*. Cell, 2014. **157**(3): p. 580-94.
9. Ikushima, H., et al., *Autocrine TGF-beta signaling maintains*

- tumorigenicity of glioma-initiating cells through Sry-related HMG-box factors*. Cell Stem Cell, 2009. **5**(5): p. 504-14.
10. Natsume, A., et al., *Chromatin regulator PRC2 is a key regulator of epigenetic plasticity in glioblastoma*. Cancer Res, 2013. **73**(14): p. 4559-70.
 11. Safa, A.R., et al., *Emerging targets for glioblastoma stem cell therapy*. J Biomed Res, 2015. **30**.
 12. Gronych, J., S.M. Pfister, and D.T. Jones, *Connect four with glioblastoma stem cell factors*. Cell, 2014. **157**(3): p. 525-7.
 13. Son, E.Y. and G.R. Crabtree, *The role of BAF (mSWI/SNF) complexes in mammalian neural development*. Am J Med Genet C Semin Med Genet, 2014. **166C**(3): p. 333-49.
 14. Hohmann, A.F. and C.R. Vakoc, *A rationale to target the SWI/SNF complex for cancer therapy*. Trends Genet, 2014. **30**(8): p. 356-63.
 15. Yaniv, M., *Chromatin remodeling: from transcription to cancer*. Cancer Genet, 2014.
 16. Middeljans, E., et al., *SS18 together with animal-specific factors defines human BAF-type SWI/SNF complexes*. PLoS One, 2012. **7**(3): p. e33834.
 17. Lessard, J., et al., *An essential switch in subunit composition of a chromatin remodeling complex during neural development*. Neuron, 2007. **55**(2): p. 201-15.
 18. Ho, L., et al., *An embryonic stem cell chromatin remodeling complex, esBAF, is essential for embryonic stem cell self-renewal and*

- pluripotency*. Proc Natl Acad Sci U S A, 2009. **106**(13): p. 5181-6.
19. Kidder, B.L., S. Palmer, and J.G. Knott, *SWI/SNF-Brg1 regulates self-renewal and occupies core pluripotency-related genes in embryonic stem cells*. Stem Cells, 2009. **27**(2): p. 317-28.
 20. Tando, T., et al., *Requiem protein links RelB/p52 and the Brm-type SWI/SNF complex in a noncanonical NF-kappaB pathway*. J Biol Chem, 2010. **285**(29): p. 21951-60.
 21. Ishizaka, A., et al., *Double plant homeodomain (PHD) finger proteins DPF3a and -3b are required as transcriptional co-activators in SWI/SNF complex-dependent activation of NF-kappaB RelA/p50 heterodimer*. J Biol Chem, 2012. **287**(15): p. 11924-33.
 22. Pastrana, E., V. Silva-Vargas, and F. Doetsch, *Eyes wide open: a critical review of sphere-formation as an assay for stem cells*. Cell Stem Cell, 2011. **8**(5): p. 486-98.
 23. Hong, S., et al., *Functional analysis of various promoters in lentiviral vectors at different stages of in vitro differentiation of mouse embryonic stem cells*. Mol Ther, 2007. **15**(9): p. 1630-9.
 24. Norrman, K., et al., *Quantitative comparison of constitutive promoters in human ES cells*. PLoS One, 2010. **5**(8): p. e12413.
 25. Palanichamy, K., et al., *Clinically Relevant Brain Tumor Model and Device Development for Experimental Therapeutics*. Journal of Analytical Oncology, 2015. **4**: p. 5-12
 26. Hironaka, N., et al., *Tax-independent constitutive IkappaB kinase activation in adult T-cell leukemia cells*. Neoplasia, 2004. **6**(3): p.

- 266-78.
27. Sun, G., et al., *Histone demethylase LSD1 regulates neural stem cell proliferation*. Mol Cell Biol, 2010. **30**(8): p. 1997-2005.
 28. Wang, Y., H.K. Liu, and G. Schütz, *Role of the nuclear receptor Tailless in adult neural stem cells*. Mech Dev, 2013. **130**(6-8): p. 388-90.
 29. Islam, M.M. and C.L. Zhang, *TLX: A master regulator for neural stem cell maintenance and neurogenesis*. Biochim Biophys Acta, 2015. **1849**(2): p. 210-6.
 30. Cui, Q., et al., *Downregulation of TLX induces TET3 expression and inhibits glioblastoma stem cell self-renewal and tumorigenesis*. Nat Commun, 2016. **7**: p. 10637.
 31. Yang, Z., et al., *MicroRNA-214 is aberrantly expressed in cervical cancers and inhibits the growth of HeLa cells*. IUBMB Life, 2009. **61**(11): p. 1075-82.
 32. O'Loghlen, A., et al., *The nuclear receptor NR2E1/TLX controls senescence*. Oncogene, 2015. **34**(31): p. 4069-77.
 33. Wu, D., et al., *Orphan nuclear receptor TLX functions as a potent suppressor of oncogene-induced senescence in prostate cancer via its transcriptional co-regulation of the CDKN1A (p21(WAF1) (/) (CIP1)) and SIRT1 genes*. J Pathol, 2015. **236**(1): p. 103-15.
 34. Qin, S., et al., *Orphan nuclear receptor TLX regulates astrogenesis by modulating BMP signaling*. Front Neurosci, 2014. **8**: p. 74.
 35. Piccirillo, S.G., et al., *Bone morphogenetic proteins inhibit the*

- tumorigenic potential of human brain tumour-initiating cells*. Nature, 2006. **444**(7120): p. 761-5.
36. Ligon, K.L., et al., *Olig2-regulated lineage-restricted pathway controls replication competence in neural stem cells and malignant glioma*. Neuron, 2007. **53**(4): p. 503-17.
37. Watanabe, H., et al., *SWI/SNF complex is essential for NRSF-mediated suppression of neuronal genes in human nonsmall cell lung carcinoma cell lines*. Oncogene, 2006. **25**(3): p. 470-9.
38. Lian, X., et al., *Robust cardiomyocyte differentiation from human pluripotent stem cells via temporal modulation of canonical Wnt signaling*. Proc Natl Acad Sci U S A, 2012. **109**(27): p. E1848-57.
39. Haraguchi, T., Y. Ozaki, and H. Iba, *Vectors expressing efficient RNA decoys achieve the long-term suppression of specific microRNA activity in mammalian cells*. Nucleic Acids Res, 2009. **37**(6): p. e43.
40. Kitamura, T., et al., *Retrovirus-mediated gene transfer and expression cloning: powerful tools in functional genomics*. Exp Hematol, 2003. **31**(11): p. 1007-14.
41. Yu, J.Y., S.L. DeRuiter, and D.L. Turner, *RNA interference by expression of short-interfering RNAs and hairpin RNAs in mammalian cells*. Proc Natl Acad Sci U S A, 2002. **99**(9): p. 6047-52.
42. Haraguchi, T., et al., *SiRNAs do not induce RNA-dependent transcriptional silencing of retrovirus in human cells*. FEBS Lett, 2007. **581**(25): p. 4949-54.

43. Yamamichi, N., et al., *The Brm gene suppressed at the post-transcriptional level in various human cell lines is inducible by transient HDAC inhibitor treatment, which exhibits antioncogenic potential*. *Oncogene*, 2005. **24**(35): p. 5471-81.
44. Gustafsdottir, S.M., et al., *Proximity ligation assays for sensitive and specific protein analyses*. *Anal Biochem*, 2005. **345**(1): p. 2-9.
45. Poulard, C., et al., *Proximity ligation assay to detect and localize the interactions of ER α with PI3-K and Src in breast cancer cells and tumor samples*. *Methods Mol Biol*, 2014. **1204**: p. 135-43.

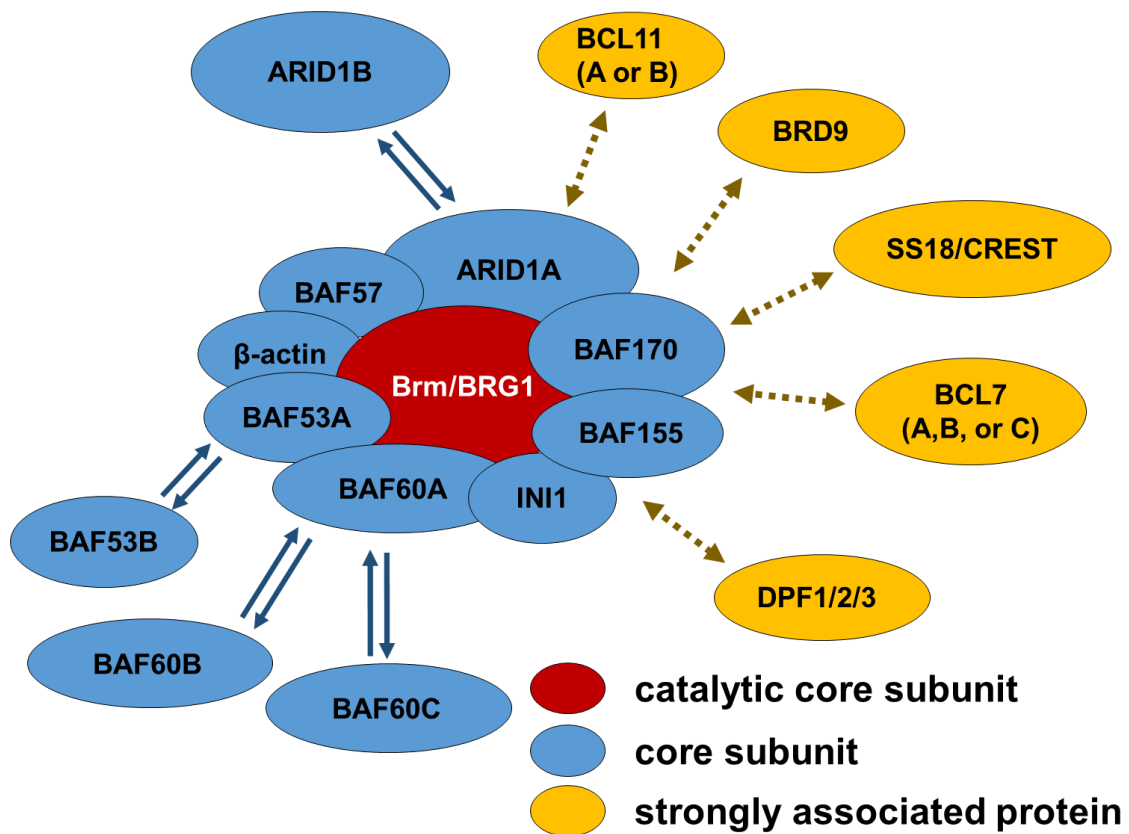


Figure 1: Schematic representation of the SWI/SNF complex. The SWI/SNF complex consists of a catalytic ATPase subunit (either BRG1 or Brm), the other core subunits and its strongly associated cofactor proteins. Some of these proteins are able to replace with another family member.

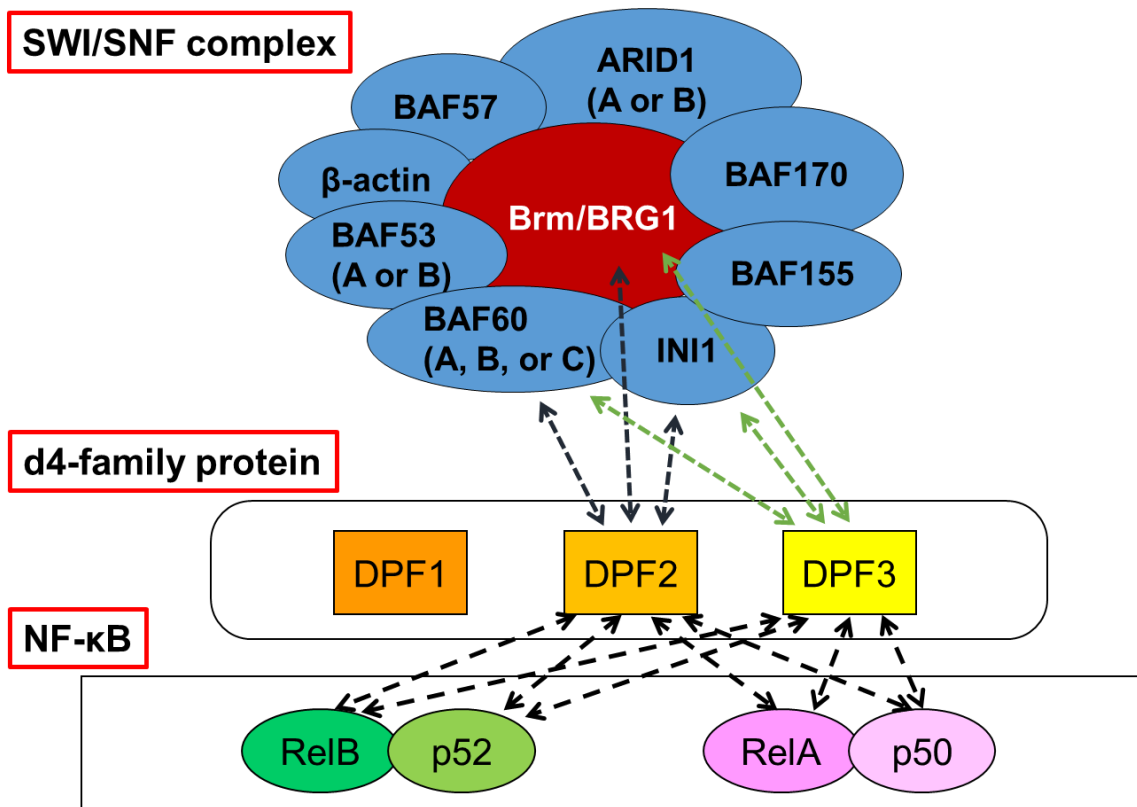


Figure 2: Schematic representation of the adapter function of d4-family proteins linking SWI/SNF complex and NF- κ B dimers in epithelial tumor cell lines. DPF2 and DPF3 directly interact with Brm/BRG1, BAF155, INI1, RelA, p50, RelB and p52. High level exogenous expression of DPF1 can also potentiate the transactivating activity of NF- κ B dimers.

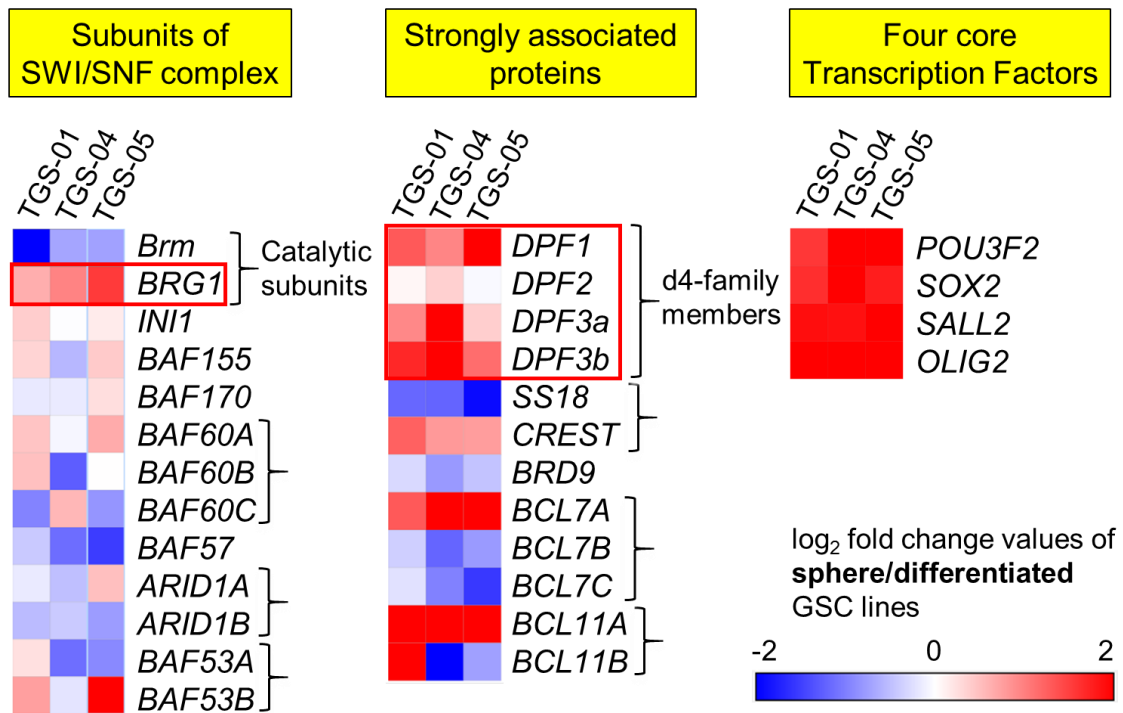


Figure 3: Expression of mRNAs encoding the subunits of SWI/SNF core complex, its strongly associated proteins and four core transcription factors in three GIC preparations and their corresponding differentiated cells. mRNA expression in sphere cultures of TGS-01, -04 or -05 were analyzed by qRT-PCR and compared with those in differentiated monolayer cultures derived from these cultures. The heat map represents the log₂ fold changes in gene expression (sphere culture/differentiated monolayer culture). Red and blue indicate higher and lower expression, respectively, in sphere cultures compared with differentiated monolayer cultures.

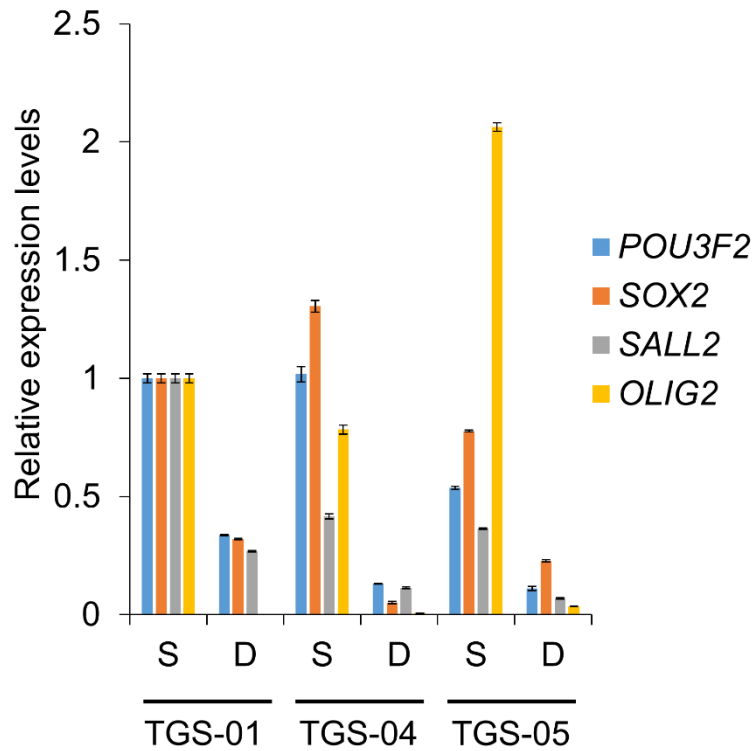


Figure 4: Specific expression of four core transcription factors in sphere cultures of GICs and in differentiated monolayer cultures derived from them. Relative gene expression levels of the four core transcription factors analyzed by qRT-PCR from the experiment described in Figure 1. Error bars represent standard deviation of the mean from triplicate experiments. S, sphere culture; D, differentiated monolayer culture.

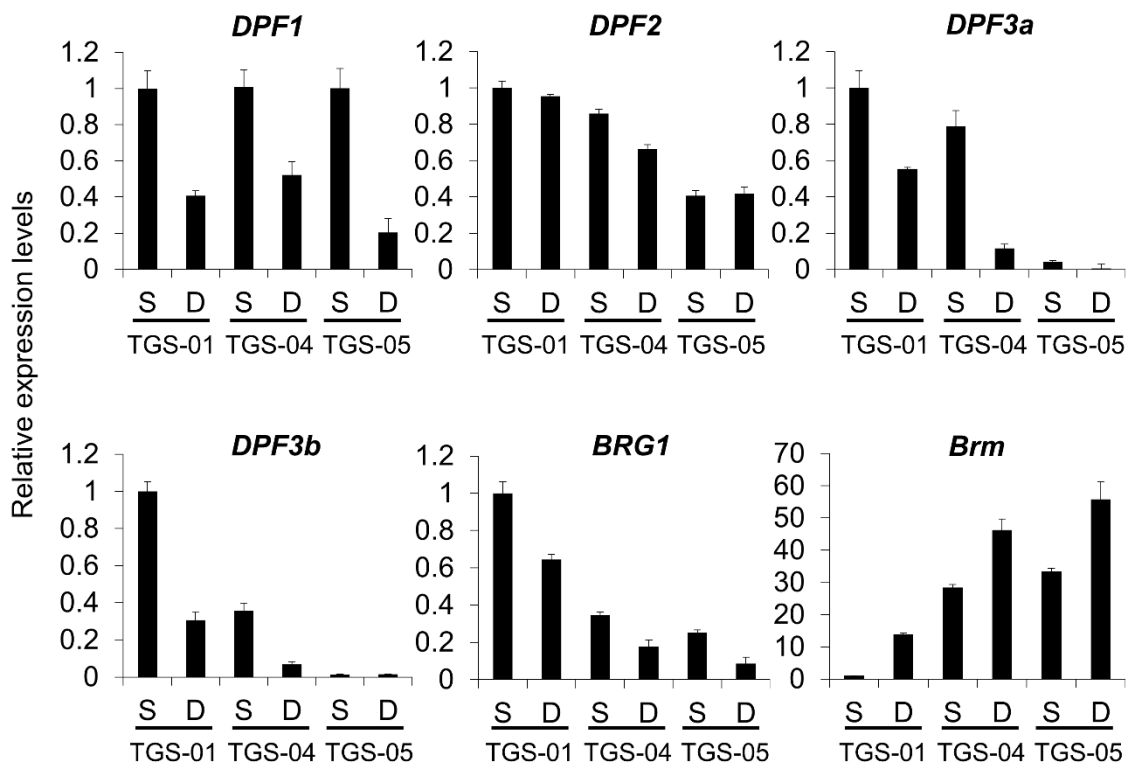


Figure 5: Expression of mRNAs encoding the subunits of SWI/SNF core complex and its strongly associated proteins in three GIC preparations and their corresponding differentiated cells. Relative gene expression levels of the d4-family members, *BRG1* and *Brm* analyzed by qRT-PCR from the experiment described in Figure 1. Error bars represent standard deviation of the mean from triplicate experiments. S, sphere culture; D, differentiated monolayer culture.

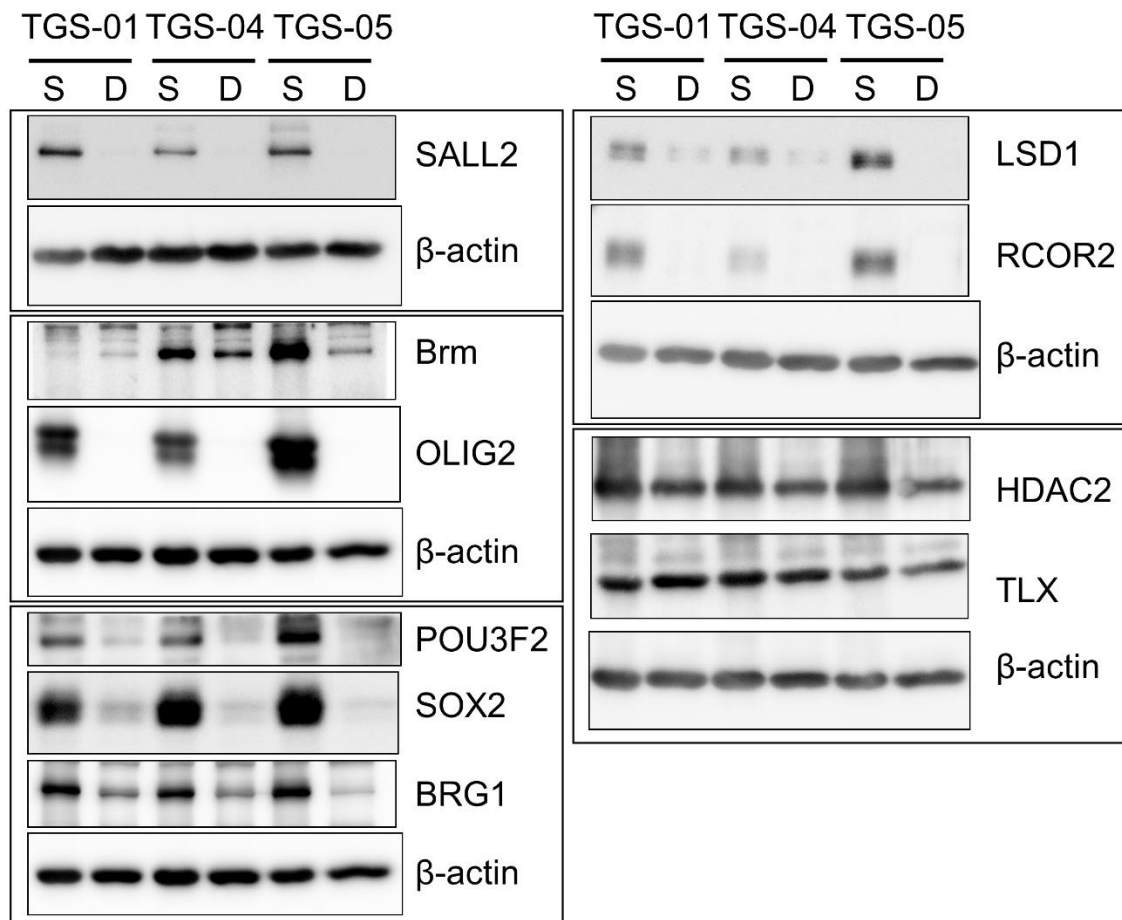


Figure 6: Expression of four core transcription factors and other proteins in sphere cultures of GICs and in differentiated monolayer cultures derived from them. Western blotting analysis of the four core transcription factors and other proteins. Blots in a black line box are originated from the same gel. The same set of protein samples was used for each blot. S, sphere culture; D, differentiated monolayer culture.

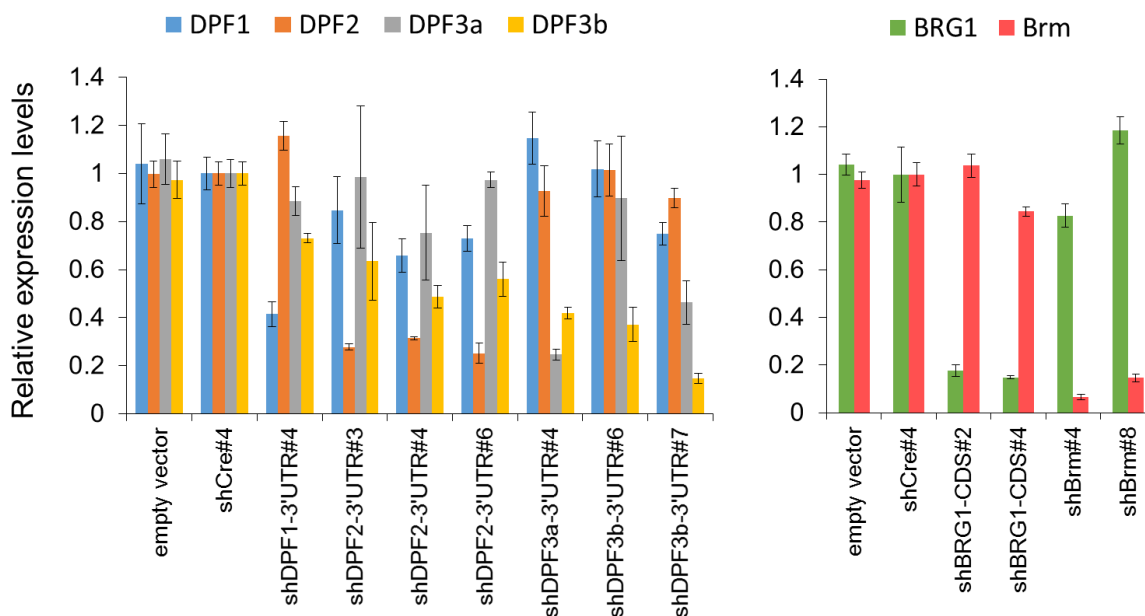


Figure 7: Suppression of mRNA levels by shRNAs designed for d4-family members, *BRG1* and *Brm*. MDA-MB-231 cells, which expresses all of the d4-family members, *BRG1* and *Brm* at significant levels were transduced with pSSSP-based retrovirus vectors expressing these shRNAs and control shRNA (shCre#4) as well as an empty vector (pSSSP [43]). mRNA levels were measured by qRT-PCR. The expression levels of cells transduced with the control vector were taken as 1.0 and error bars represent standard deviation of the mean from triplicate experiments.

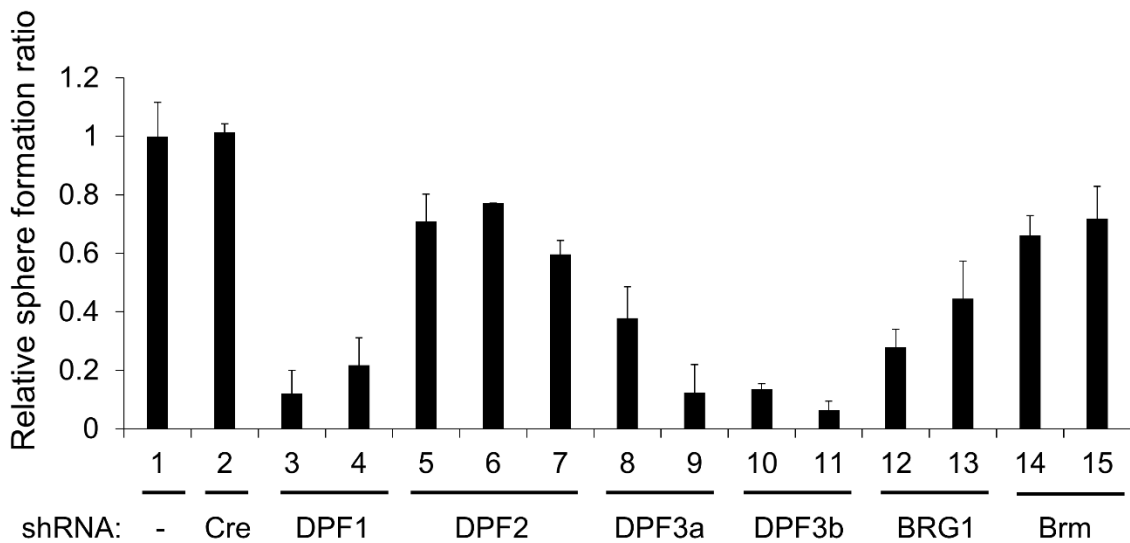


Figure 8: Knockdown effects of d4-family members, *BRG1* or *Brm* on the sphere forming activity of GICs. Relative sphere formation ratio of TGS-01 cells transduced with retrovirus vectors expressing various shRNAs or empty vector (EV-1; lane1); shCre#4 (lane 2), shDPF1-CDS#1 (lane 3), shDPF1-3'UTR#4 (lane 4), shDPF2-3'UTR#3, #4 and #6 (lanes 5-7), shDPF3a-3'UTR#2 (lane 8), and shDPF3a-3'UTR#4 (lane 9), shDPF3b-CDS#6 and #7 (lanes 10, 11), shBRG1-CDS#2 and #4 (lanes 12, 13) and shBrm#4, and #8 (lanes 14, 15). Error bars represent standard deviation of the mean from triplicate experiments.

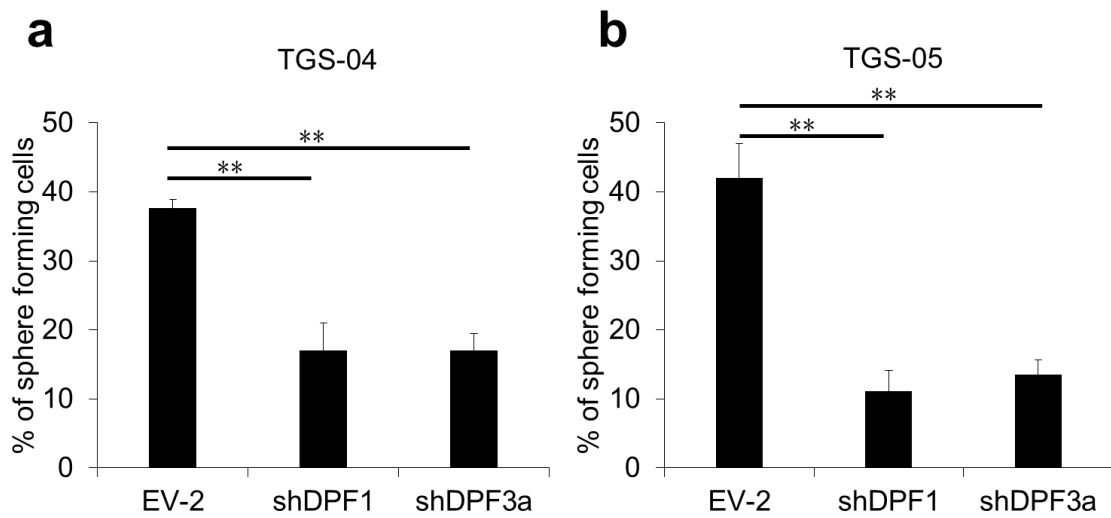


Figure 9: Effects of *DPF1* and *DPF3a* knockdowns on sphere forming activity in GICs. Percentage of sphere forming cells in TGS-04 (a) and TGS-05 (b) cultures transduced with lentivirus based on pLE-IG expressing shDPF1-3'UTR#4 or shDPF3a-3'UTR#4 or empty vector (EV-2). Error bars represent standard deviation of the mean from triplicate experiments. ** $p < 0.01$ by Student's t-test.

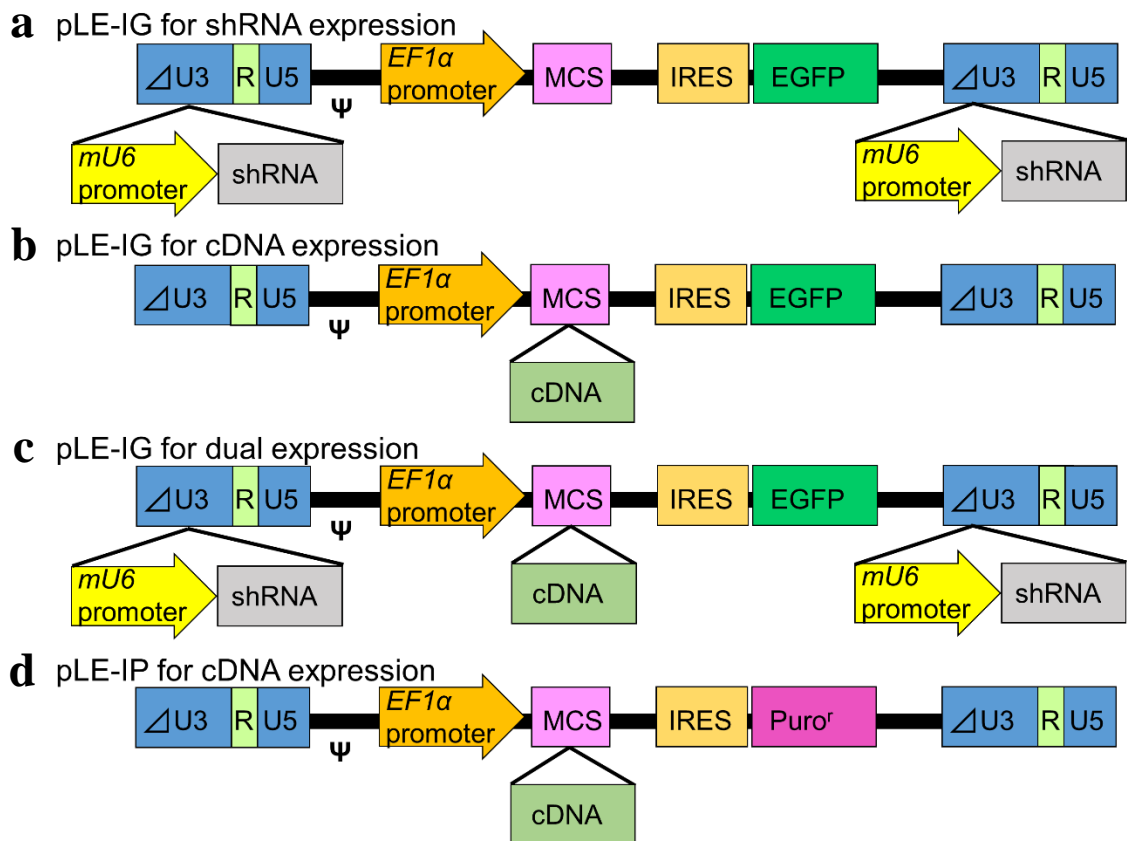


Figure 10: Proviral structures of the dual lentiviral vectors, pLE-IG and pLE-IP, simultaneously expressing shRNA and the corresponding mRNA. Proviral structures of the dual lentiviral vectors; pLE-IG (a, b, c) and pLE-IP (d). mRNA expression is driven by the *EF1 α* pol II promoter, whereas that of shRNA is driven by *mU6* pol III promoter. Each mRNA was designed to be resistant to the corresponding shRNA. pLE-IG and pLE-IP vectors that lack the cDNA insertion (a) or shRNA expression unit (b, d) were also used to express only mRNA or shRNA, respectively. Empty vectors (EV-2; pLE-IG, EV-3; pLE-IP) have neither the cDNA nor shRNA expression unit. Δ U3, the U3 sequence from which major enhancer sequences were deleted; R, lentiviral R sequence; U5, lentiviral U5 sequence; Ψ , lentiviral packaging signal.

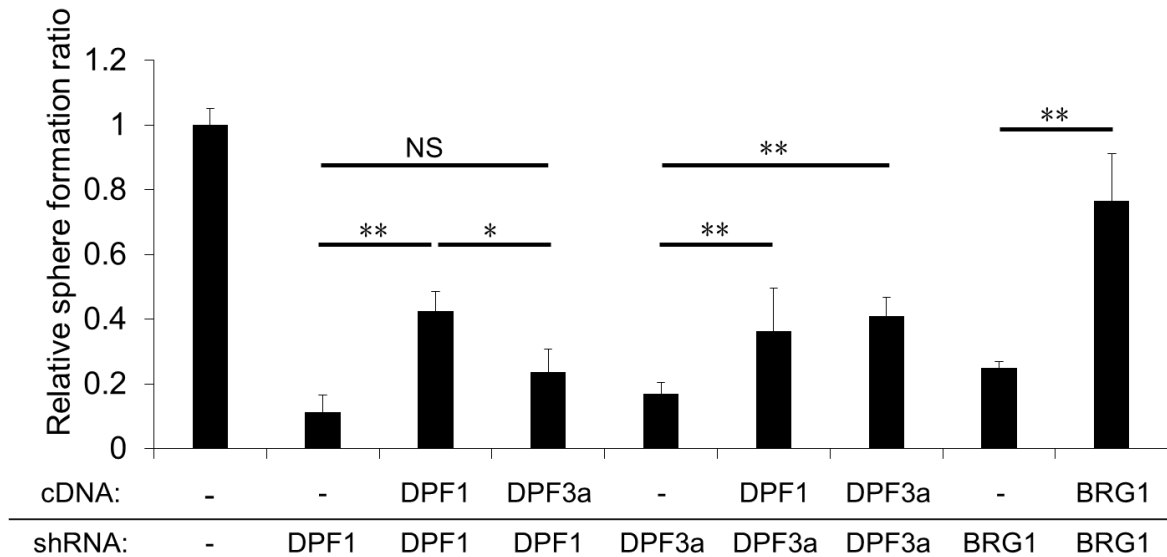


Figure 11: Knockdown and rescue experiments using dual expression vectors. Relative sphere formation ratio of TGS-01 cells transduced with the dual lentivirus vectors based on pLE-IG simultaneously expressing mRNA (3×FLAG-DPF1, -DPF3a and -BRG1) and shRNA (shCre#4, shDPF1-3'UTR#4, shDPF3a-3'UTR#4, shBRG1-CDS#2) for the rescue experiments. Similar results were obtained from at least two independent experiments. Error bars represent standard deviation of the mean from triplicate experiments. NS = not significant, * $p < 0.05$, ** $p < 0.01$ by Student's t-test.

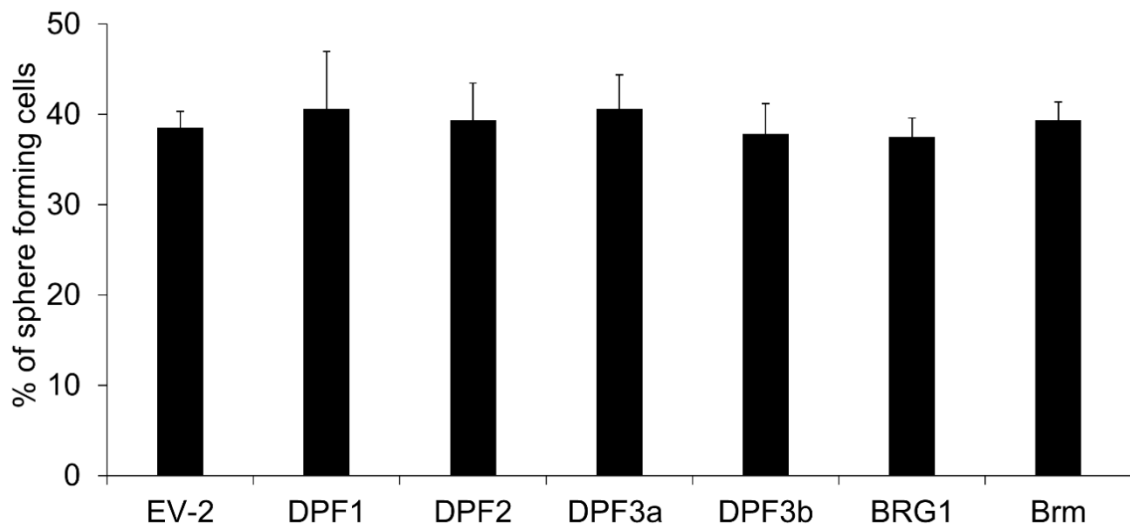


Figure 12: Effects of exogenous d4-family proteins, BRG1 and Brm expression on the sphere forming activity of TGS-01 cells. Percentage of sphere forming TGS-01 cells transduced with lentivirus based on pLE-IG expressing d4-family proteins or BRG1, or with an empty vector (EV-2). Error bars represent the standard deviation of the mean from triplicate experiments.

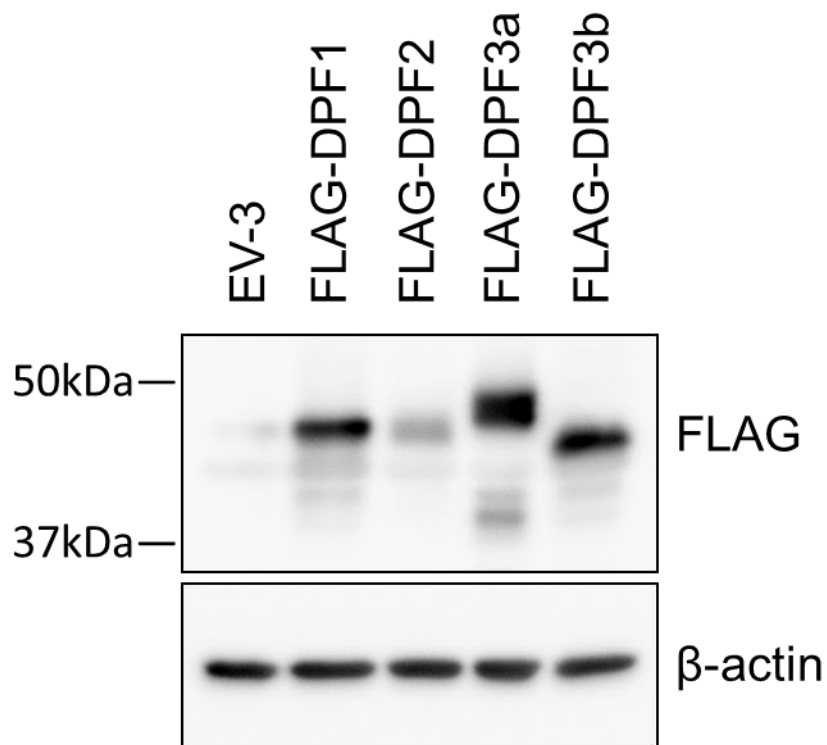


Figure 13: Expression levels of exogenously introduced d4-family proteins. TGS-01 cells were transduced with lentivirus vectors based on pLE-IP expressing d4-family proteins as well as an empty vector (EV-3). These cell lysates were analyzed by western blotting using anti-FLAG antibody. β -actin was used as the loading control.

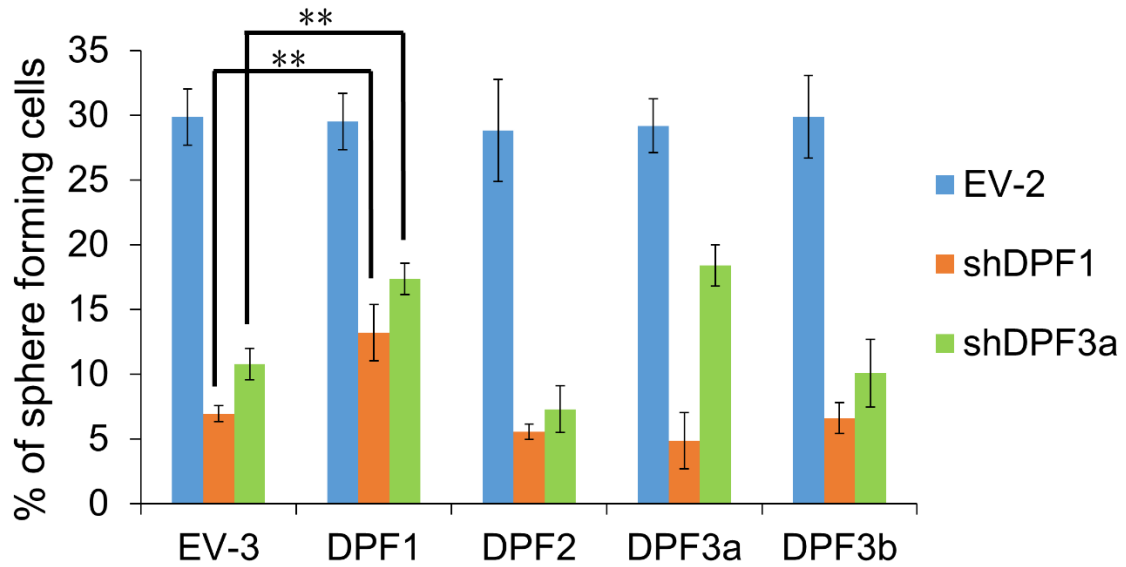


Figure 14: Effects of *DPF1* and *DPF3a* knockdowns on the sphere forming activity of TGS-01 cells exogenously expressing d4-family proteins. TGS-01 cells transduced with lentivirus vectors based on pLE-IP expressing d4-family proteins as well as an empty vector (EV-3) were additionally transduced with lentivirus vectors based on pLE-IG expressing shDPF1-3'UTR#4, shDPF3a-3'UTR#4, or shBRG1-CDS#2 as well as an empty vector (EV-2). Error bars represent standard deviation of the mean from triplicate experiments. ** $p < 0.01$ by Student's t-test.

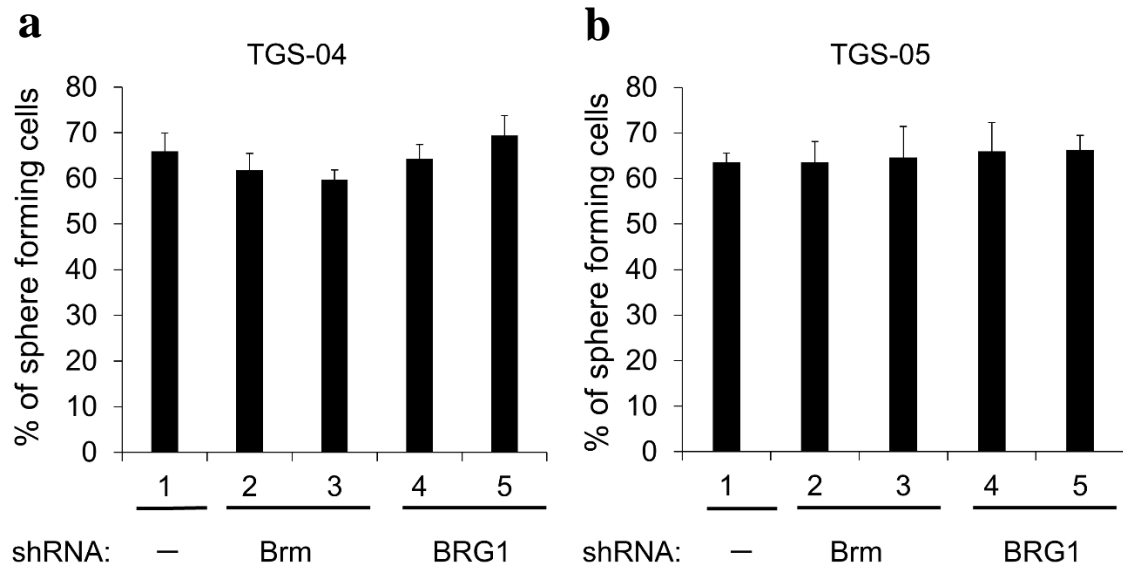


Figure 15: Effects of a *BRG1* or *Brm* knockdown on the sphere forming activity of TGS-04 and TGS-05 cells. Percentage of sphere forming cells in TGS-04 (a) and TGS-05 (b) cultures transduced with lentivirus vectors based on pLE-IG expressing shBrm or shBRG1 or empty vector (EV-2; lane 1); shBrm#4, and #8 (lanes 2, 3) and shBRG1-CDS#2 and #4 (lanes 4, 5). Error bars represent standard deviation of the mean from triplicate experiments.

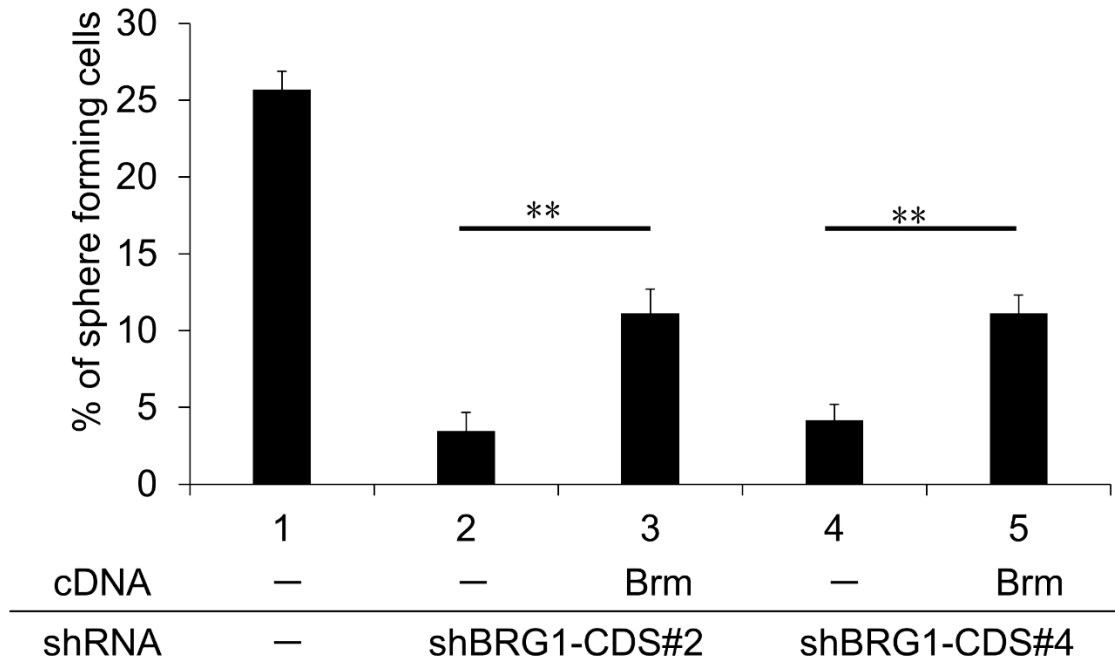


Figure 16: *BRG1* knockdown and rescue experiments using dual expression vectors. Percentage of sphere forming cells in TGS-01 cultures transduced with the dual lentivirus vectors based on pLE-IG expressing 3×FLAG-Brm and shBRG1 simultaneously for the rescue experiments. Lanes 2 and 4 are shBRG1-CDS#2, and lanes 3 and 5 are shBRG1-CDS#4. Error bars represent standard deviation of the mean from triplicate experiments. **p < 0.01 by Student’s t-test.

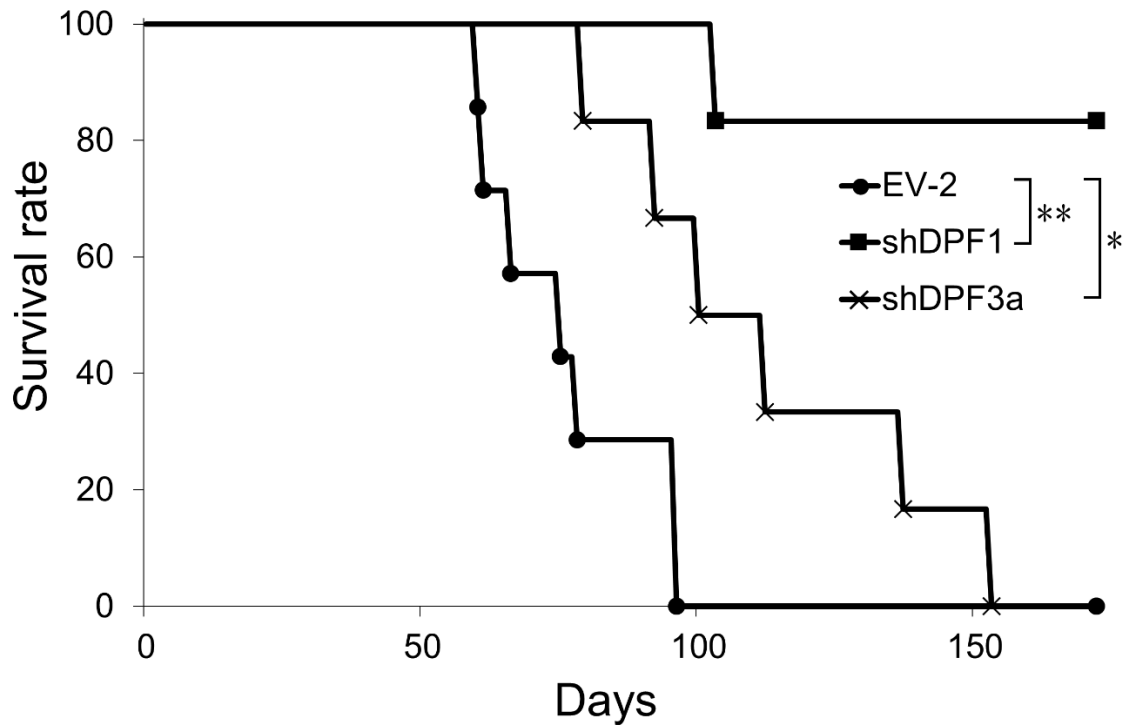


Figure 17: Kaplan-Meier survival curves of mice orthotopically injected with TGS-01 cells. TGS-01 cells transduced (3×10^3 cells in each case) with lentivirus vectors based on pLE-IG expressing shDPF1-3'UTR#4 or shDPF3a-3'UTR#4 or empty vector (EV-2) were sorted by flow cytometry two days after the transduction and injected into the cerebral hemisphere of 6-week-old female nude mice. * $p < 0.05$, ** $p < 0.01$ by log-rank test.

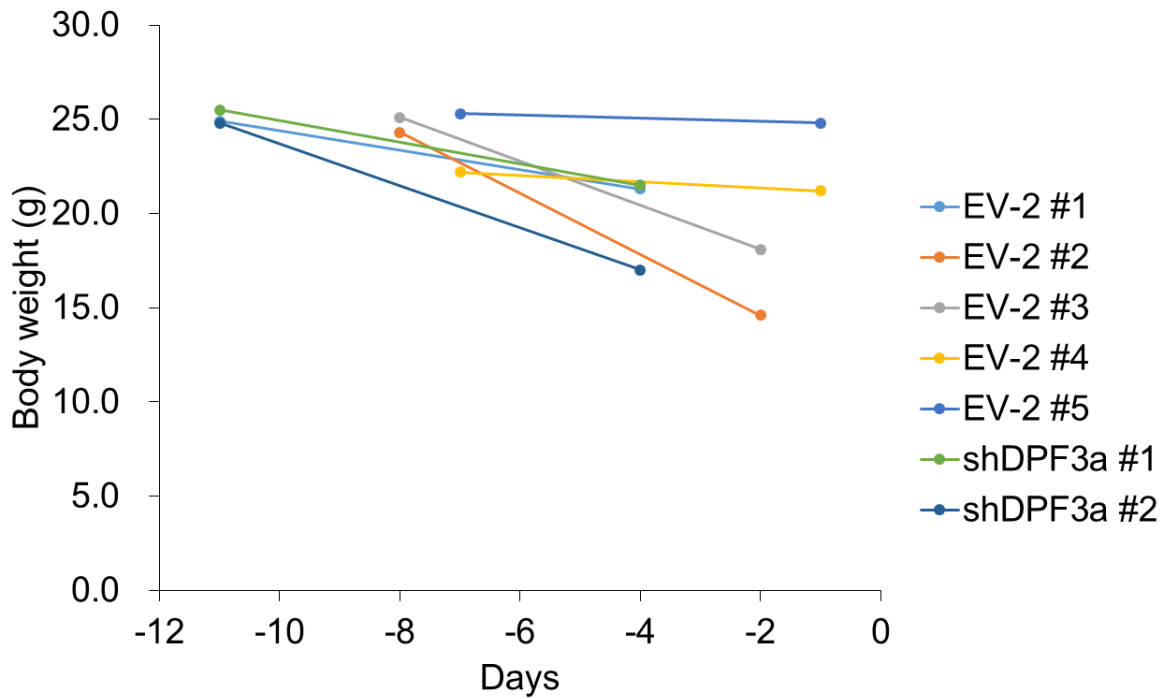


Figure 18: Body weight loss of the mice measured during 1-4 days before death. Body weights of 7 mice used in Figure 17 were measured during 1-4 days before the death (day 0). They were compared with those measured at the previous time point. #1-5 are identification numbers of the mice.

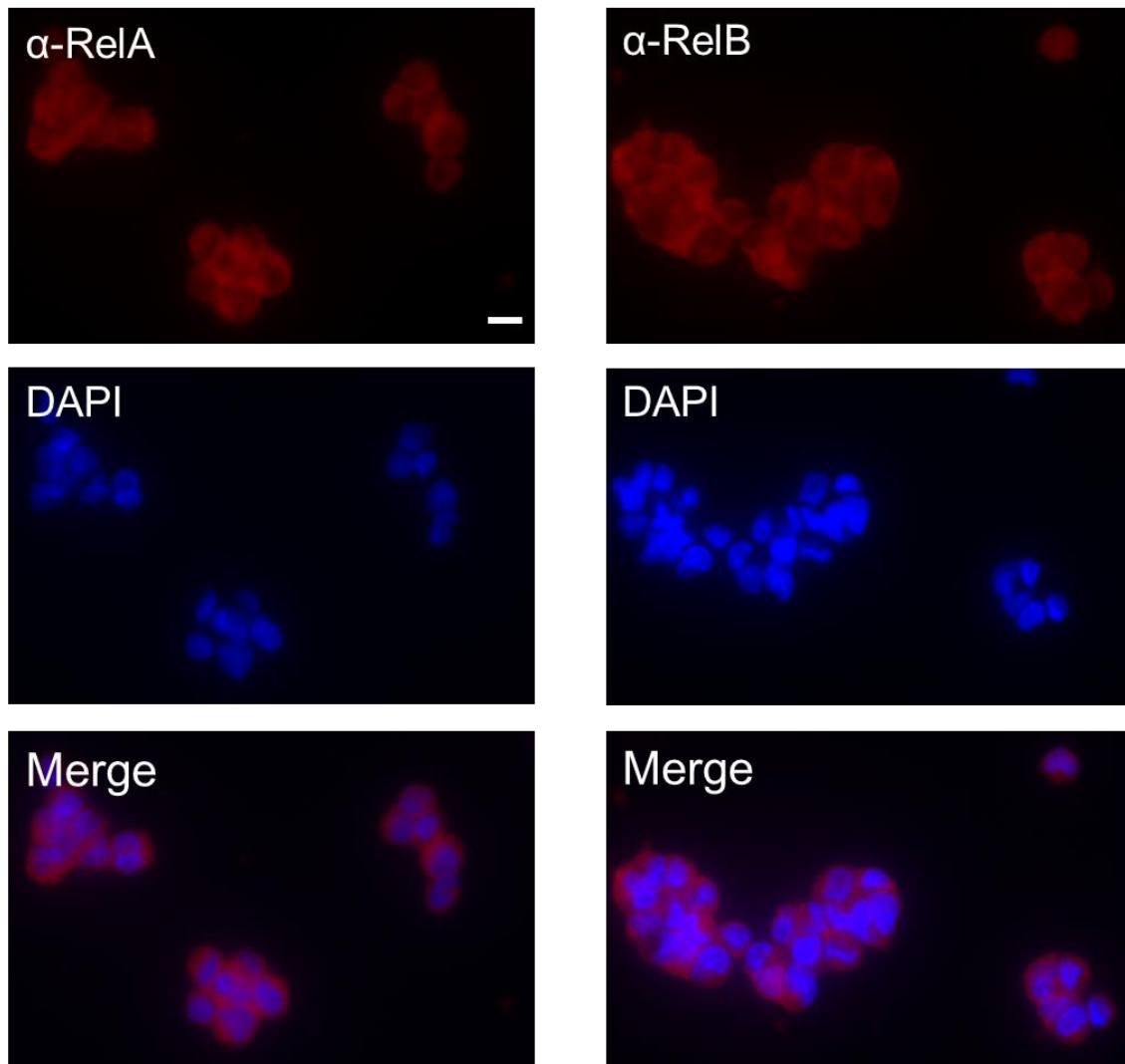


Figure 19: Subcellular localization of RelA and RelB in sphere cultures of TGS-01. Immunofluorescent assays were performed to detect RelA and RelB in TGS-01 cells. Nuclei were counterstained with DAPI. Scale bar indicates 10 μm .

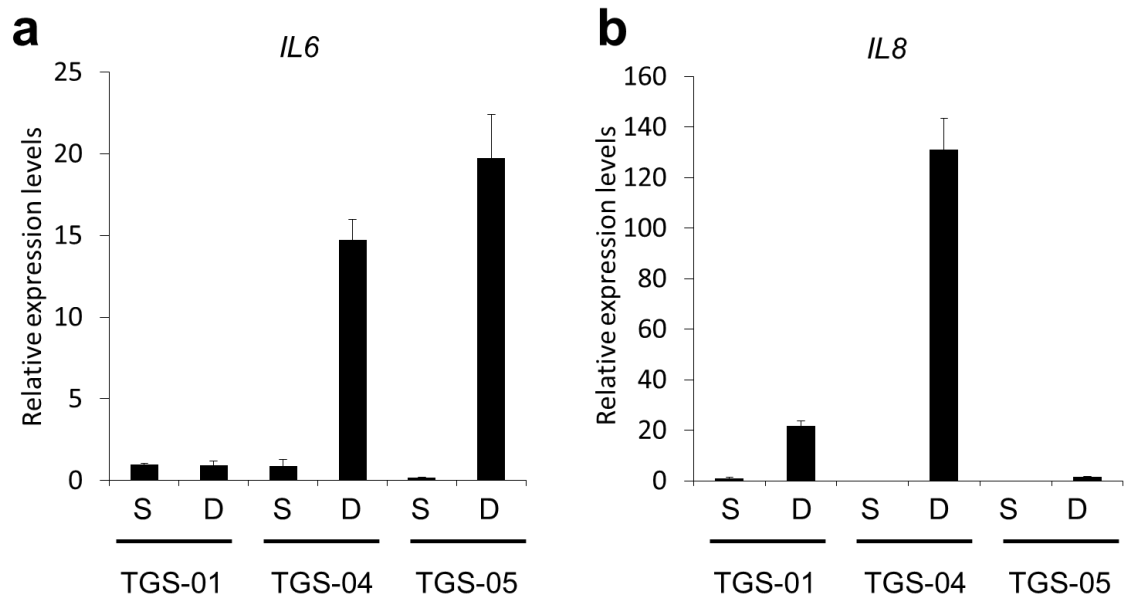


Figure 20: Expression patterns of representative SWI/SNF-dependent NF- κ B target genes in sphere cultures of GICs and in differentiated monolayer cultures derived from them. The expression levels of *IL6* (a), and *IL8* (b) in both sphere and differentiated monolayer cultures of GICs were analyzed by qRT-PCR and compared. Error bars represent the standard deviation of the mean from triplicate experiments.

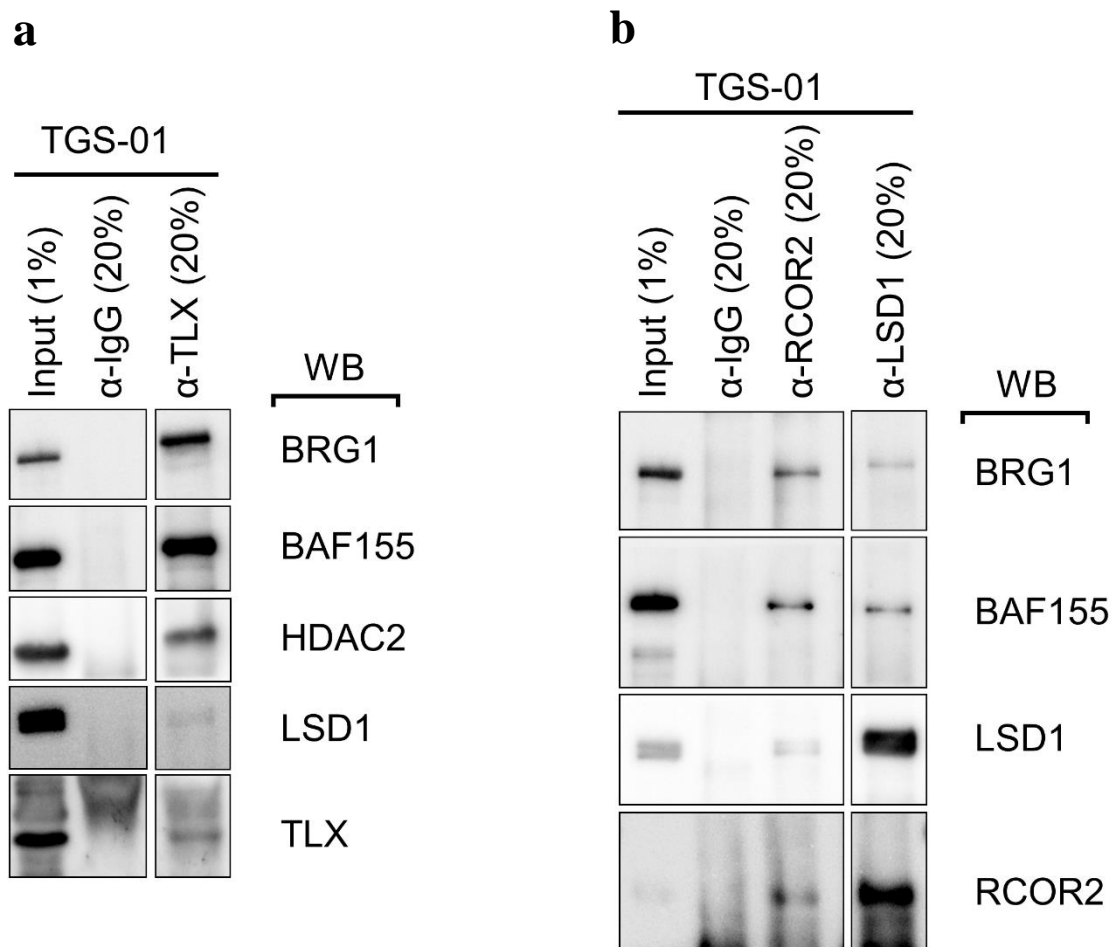


Figure 21: Detection of larger SWI/SNF complexes that include TLX and LSD1/RCOR2 in GICs. Coimmunoprecipitation of SWI/SNF complex subunits with corepressor complex. TGS-01 lysates were immunoprecipitated with anti-TLX (a) or anti-LSD1 and anti-RCOR2 (b) antibodies, and the resulting immunoprecipitates were analyzed by western blotting. The samples were derive from the same experiment and the gels/blots were processed in parallel.

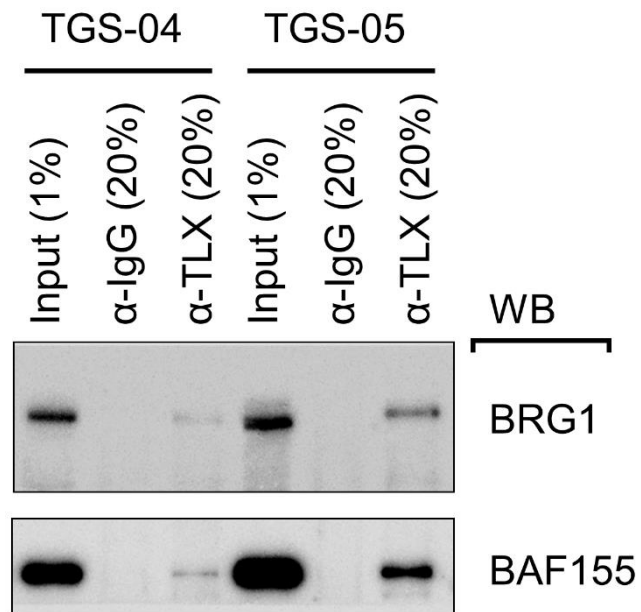


Figure 22: Detection of SWI/SNF complex/TLX interactions in GICs. TGS-04 and TGS-05 lysates were immunoprecipitated with TLX antibodies and the resulting immunoprecipitates were analyzed by western blotting.

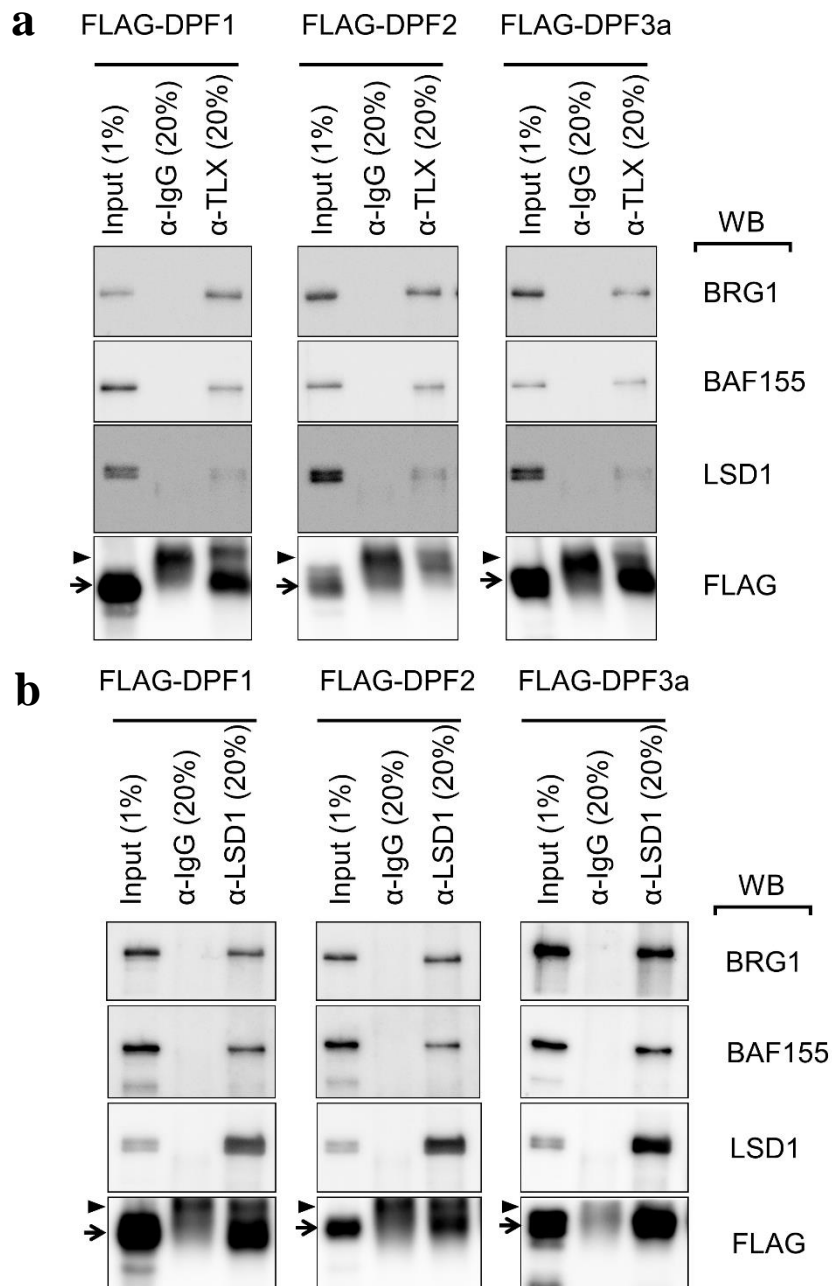


Figure 23: Detection of interactions between d4-family proteins and larger SWI/SNF complexes that include TLX and LSD1/RCOR2. TGS-01 cells exogenously expressing 3×FLAG-DPF1, -DPF2 or -DPF3a lysates were immunoprecipitated with anti-TLX antibody (a) or anti-LSD1 antibody (b), and the immunoprecipitates were analyzed by western blotting. Arrows, FLAG-tagged d4-family proteins; arrowheads, IgG heavy chains.

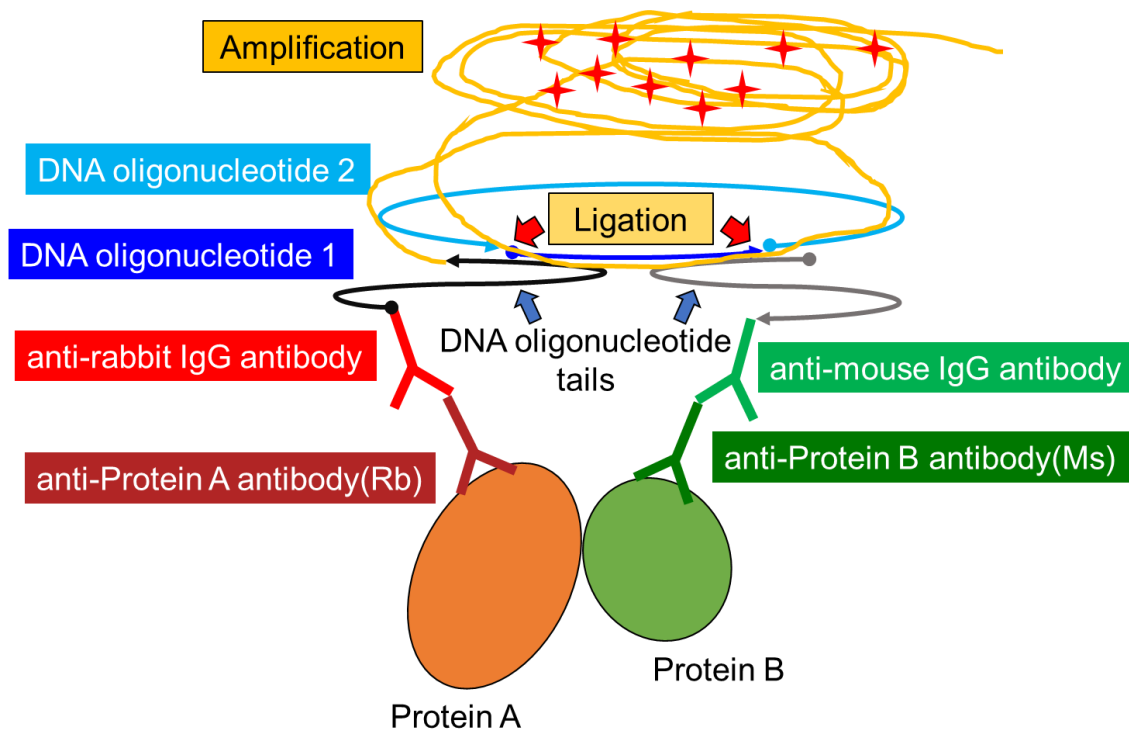


Figure 24: Schematic representation of in situ proximity ligation assay (PLA). Two primary antibodies raised in different species (rabbit; Rb and mouse; Ms in this study) recognize the each target protein (Protein A or Protein B). Species-specific secondary antibodies (PLA probes), each with a unique short DNA strand (DNA oligonucleotide tail) attached to it, bind to the primary antibodies. When the PLA probes are in close proximity (<40 nm), the DNA strands can interact through a subsequent addition of two other circle-forming DNA oligonucleotides. Several-hundredfold replication of the DNA circle can occur after the amplification reaction, and a fluorescent signal is generated by labelled complementary oligonucleotide probes. Each detected signal is visualized as an individual fluorescent dot when viewed with a fluorescence microscope [44, 45].

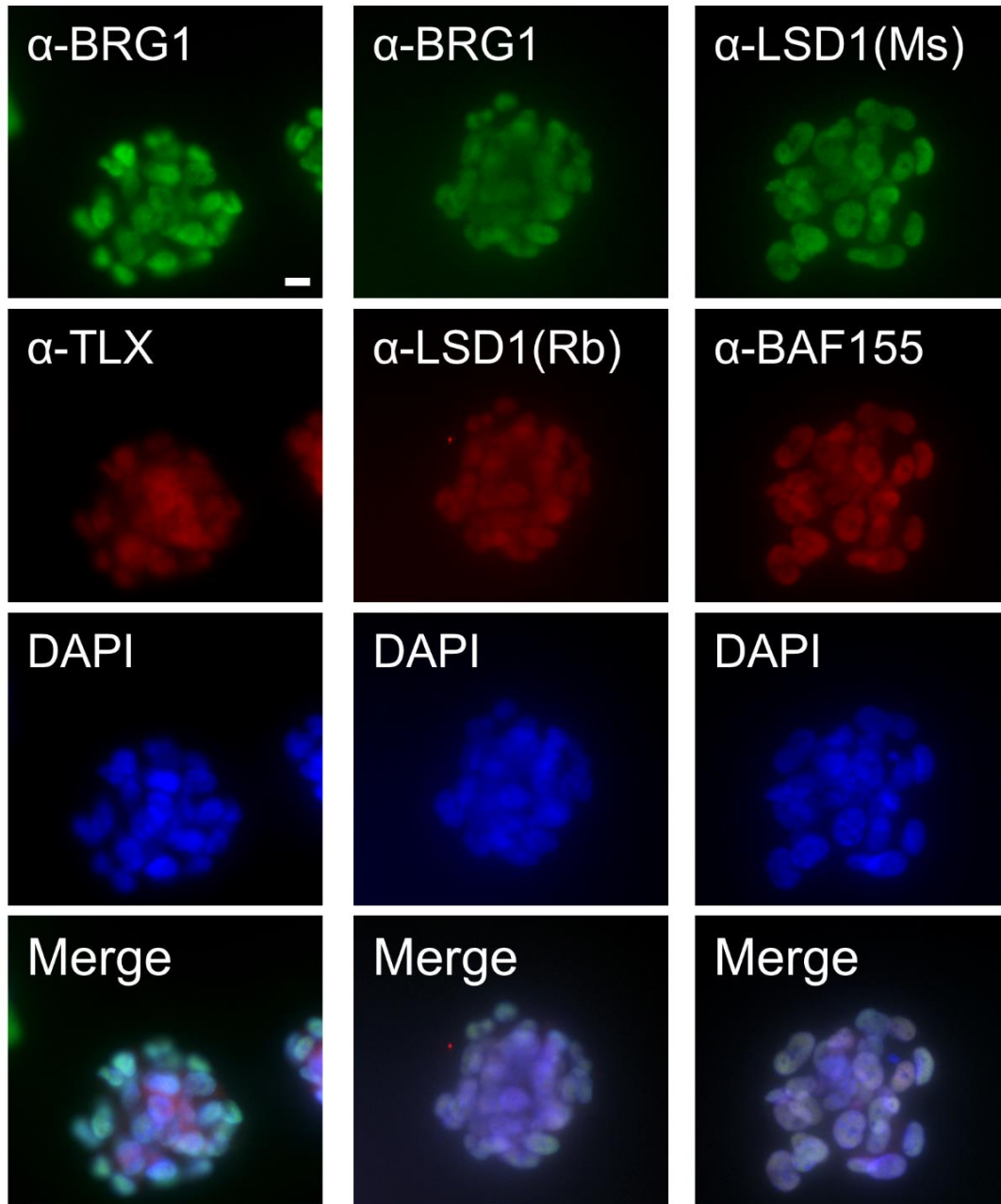


Figure 25: Subcellular localization of BRG1, BAF155, TLX and LSD1.

Immunofluorescent assays were performed to detect BRG1, TLX, LSD1 and BAF155 in TGS-01 cells. The antibodies used were as described for the PLA experiments in Figure 18. Nuclei were counterstained with DAPI. Scale bar indicates 10 μ m. Rb; rabbit, Ms; mouse.

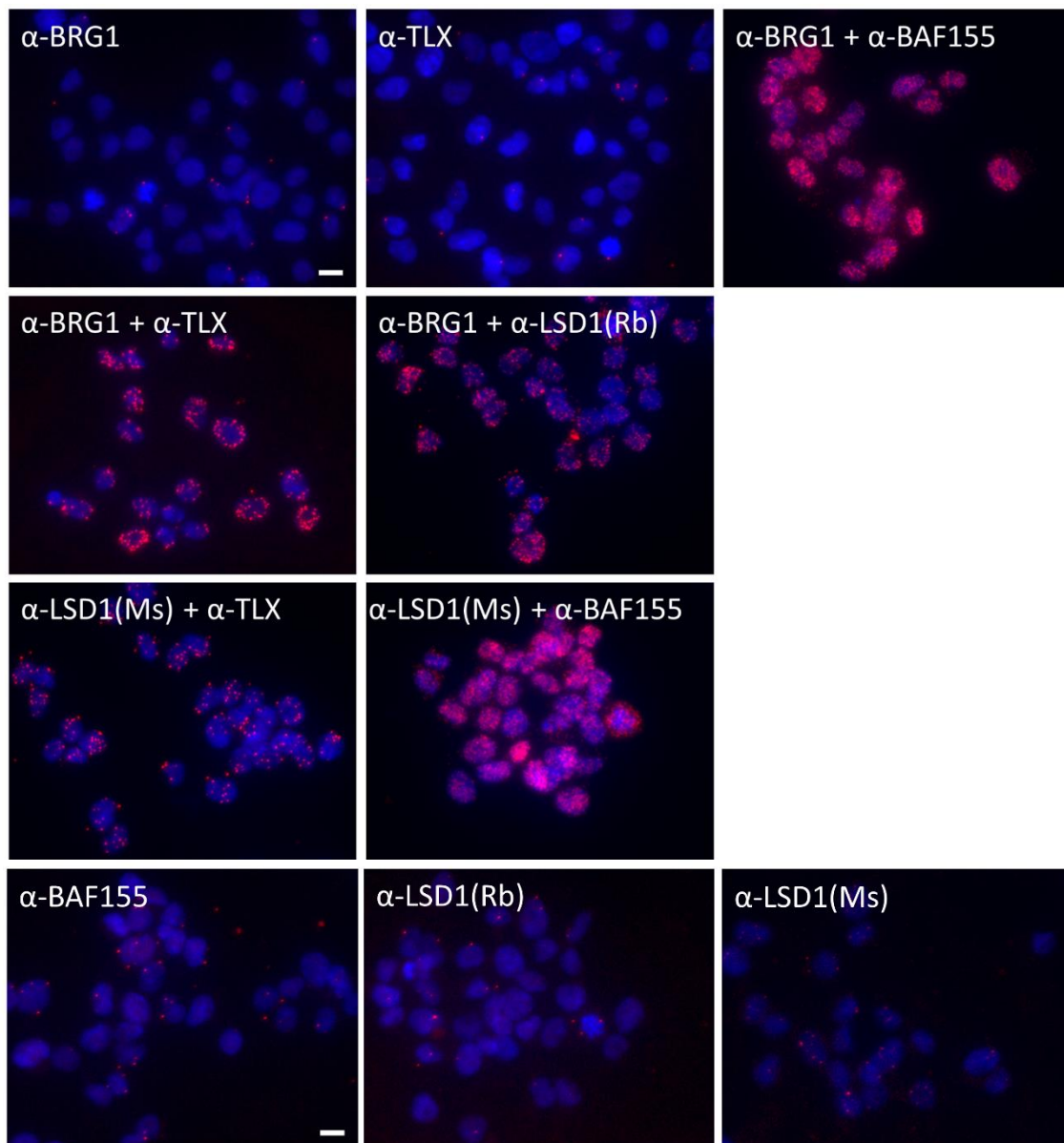


Figure 26: Proximal localization of the SWI/SNF core complex, TLX and LSD1/RCOR2 in TGS-01 cells as detected by PLA. TGS-01 cells were fixed and incubated with a single antibody or pairs of antibodies. Red dots indicate interactions and nuclei were counterstained with DAPI (blue). The red fluorescence images were obtained using quick-full-focus function of the BZ-X710 (Keyence) at depth of about 10 μm . Scale bar indicates 10 μm . Rb; rabbit, Ms; mouse.

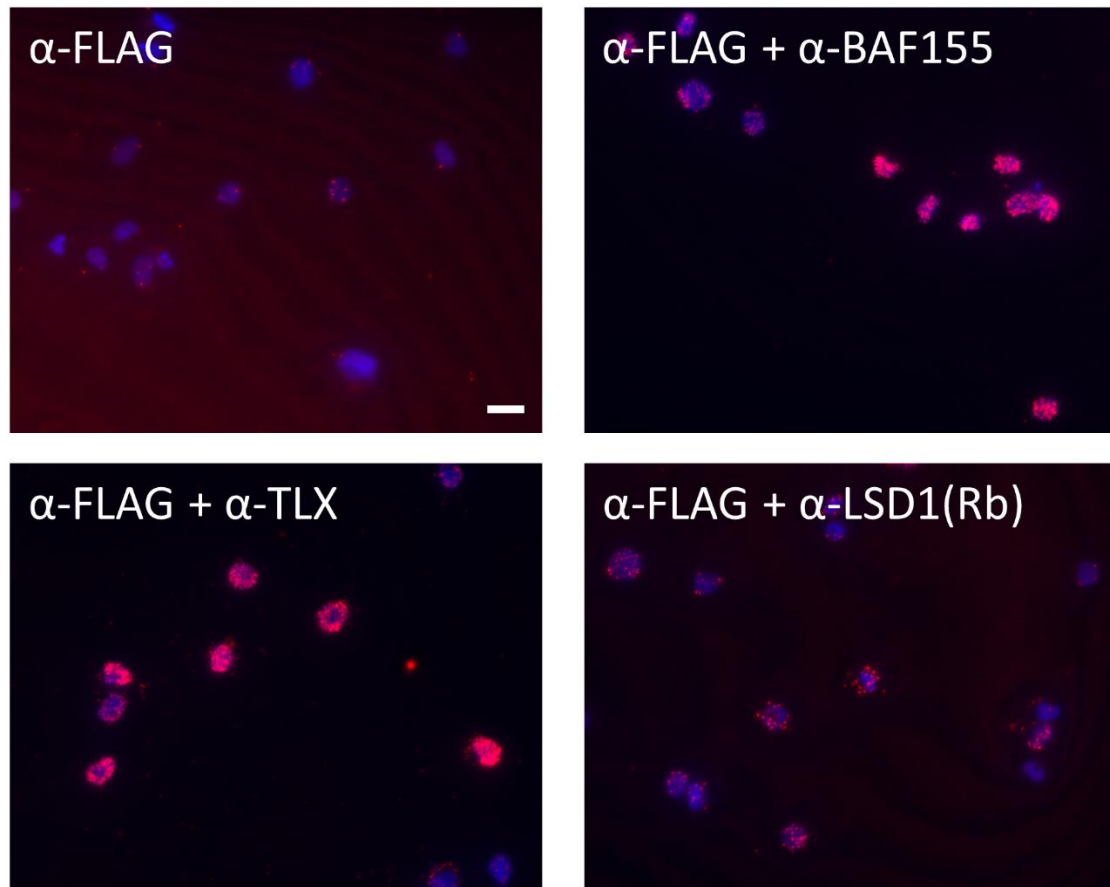


Figure 27: Proximal localization of DPF1 and TLX, LSD1 or BAF155 in TGS-01 cells exogenously expressing 3×FLAG-DPF1 as detected by PLA. TGS-01 cells exogenously expressing 3×FLAG-DPF1 were fixed and incubated with a single or pair of antibodies. Red dots indicate interactions and nuclei were counterstained with DAPI (blue). The red fluorescence images were obtained using quick-full-focus function of the BZ-X710 (Keyence) at depth of about 10 μm . Scale bar indicates 10 μm .

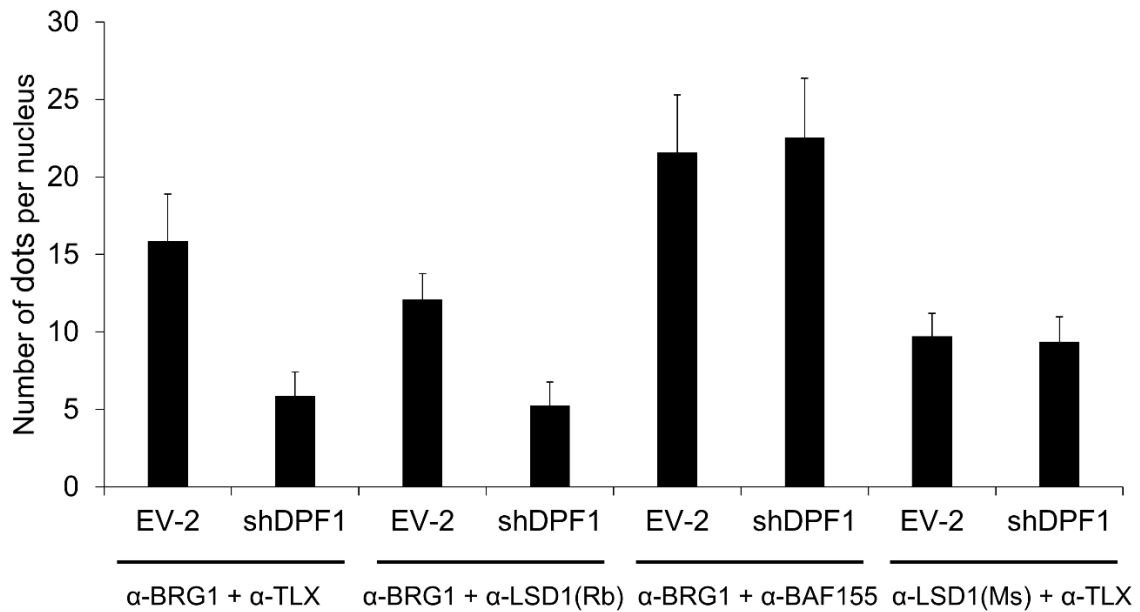


Figure 28: Effects of a *DPF1* knockdown on the proximal localization of SWI/SNF core complex, TLX and LSD1/RCOR2 in TGS-01 cells as detected by PLA. TGS-01 cells transduced with lentivirus vectors based on pLE-IG expressing shDPF1-3'UTR#4 or an empty vector (EV-2) were fixed three days after the transduction and incubated with pairs of antibody. The number of dots per nucleus of GFP positive cells was counted. Error bars represent 95% confidence intervals of the mean (N = 50).

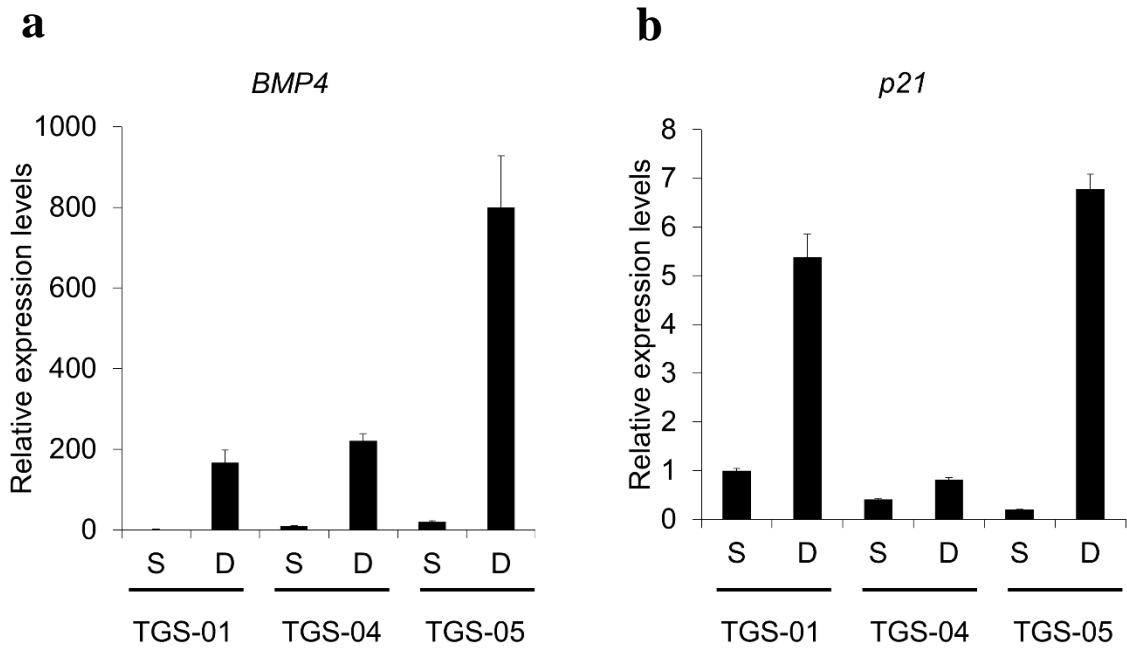


Figure 29: Expression patterns of TLX target genes in sphere cultures of GICs and in differentiated monolayer cultures derived from them. The expression levels of *BMP4* (a), and *p21* (b) in both sphere and differentiated monolayer cultures of TGS-01 were analyzed by qRT-PCR and compared. Error bars represent the standard deviation of the mean from triplicate experiments.

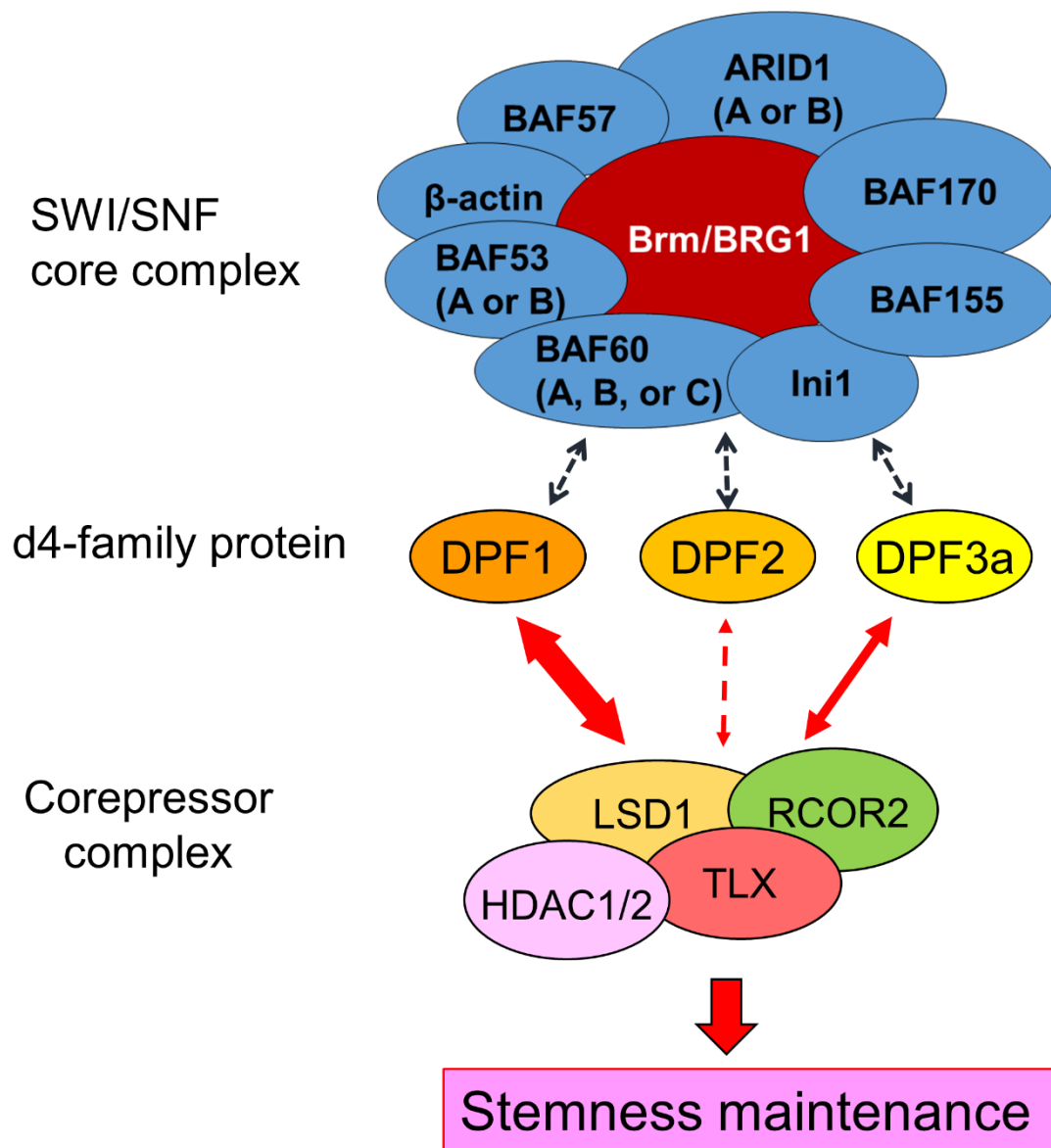


Figure 30: Schematic representation of the model of formation of a larger SWI/SNF complex that is required for stemness maintenance of GICs. The SWI/SNF core complex and a corepressor complex containing TLX, RCOR2, LSD1 and HDAC2 are linked through d4-family proteins and form a large complex.

Table 1. List of primer pairs used for plasmid constructions.

shDPF1-3'UTR#4-sense	5'-TTTGAATTAAGTGTCTGTGTATGCTTCCTGTCACA TACACAGAACAAGTTAATTCTTTTTTG-3'
shDPF1-3'UTR#4-antisense	5'-AATTCAAAAAAGAATTAAGTGTCTGTGTATGTGA CAGGAAGCATAACAGAACAAGTTAATT-3'
shDPF2-3'UTR#3-sense	5'-TTTGTAGCTTCACCTTGTATTCCGCTTCCTGTCACG GAATAACAAGGTGAAGCTACTTTTTTG-3'
shDPF2-3'UTR#3-antisense	5'-AATTCAAAAAAGTAGCTTCACCTTGTATTCCGTGA CAGGAAGCGGAATAACAAGGTGAAGCTA-3'
shDPF2-3'UTR#4-sense	5'-TTTGCTCTTAAGTGAATTGGGAGCGCTTCCTGTCAC GCTCCAATTCAGTTAAGAGCTTTTTTG-3'
shDPF2-3'UTR#4-antisense	5'-AATTCAAAAAAGCTCTTAAGTGAATTGGGAGCGTGA CAGGAAGCGCTCCAATTCAGTTAAGAG-3'
shDPF2-3'UTR#6-sense	5'-TTTGGTGATCACAGGGTTCAAACAGCTTCCTGTCAC TGTTTGAACCCTGTGATCACCTTTTTTG-3'
shDPF2-3'UTR#6-antisense	5'-AATTCAAAAAAGGTGATCACAGGGTTCAAACAGTG ACAGGAAGCTGTTTGAACCCTGTGATCAC-3'
shDPF3a-3'UTR#4-sense	5'-TTTGAAATCGAAGCAATATCCTGTGCTTCCTGTCAC ACAGGATATTGCTTCGATTTCTTTTTTG-3'
shDPF3a-3'UTR#4-antisense	5'-AATTCAAAAAAGAAATCGAAGCAATATCCTGTGTG ACAGGAAGCACAGGATATTGCTTCGATTT-3'
shDPF3b-3'CDS#6-sense	5'-TTTGGGAAGTCTCAAAGAGAAAGGCTTCCTGTCAC CTTCTCTTTGAGCAGTTCCTTTTTTG-3'
shDPF3b-3'CDS#6-antisense	5'-AATTCAAAAAAGGGAAGTCTCAAAGAGAAAGGTG ACAGGAAGCCTTCTCTTTGAGCAGTTC-3'
shDPF3b-3'CDS#7-sense	5'-TTTGATGACCAGCTACTCTTCTGCGCTTCCTGTCACG CAGAAGAGTAGCTGGTCATCTTTTTTG-3'
shDPF3b-3'CDS#7-antisense	5'-AATTCAAAAAAGATGACCAGCTACTCTTCTGCGTGA CAGGAAGCGCAGAAGAGTAGCTGGTCAT-3'
shBrm#8-sense	5'-TTTGTGATAAACTACAAAGATAGGGCTTCCTGTCAC CCTATCTTTGTAGTTTATCACTTTTTTG-3'
shBrm#8-antisense	5'-AATTCAAAAAAGTGATAAACTACAAAGATAGGGTG ACAGGAAGCCCTATCTTTGTAGTTTATCA-3'
shBRG1-CDS#2-sense	5'-TTTGTGGAAAGTACATGATTGTGGGCTTCCTGTCAC CCACAATCATGTAAGTCCAACTTTTTTG-3'

shBRG1-CDS#2-antisense	5'-AATTCAAAAAAGTTGGAAGTACATGATTGTGGGTG ACAGGAAGCCCACAATCATGTACTTCCAA-3'
shBRG1-CDS#4-sense	5'-TTTGCGTATCGCGGCTTTAAATACGCTTCCTGTCACG TATTTAAAGCCGCGATACGCTTTTTTG-3'
shBRG1-CDS#4-antisense	5'-AATTCAAAAAAGCGTATCGCGGCTTTAAATACGTGA CAGGAAGCGTATTTAAAGCCGCGATACG-3'
EF1 α -Fwd	5'-GTTTAAACGCCACAAATGGCAGTATTCATCCA-3'
EF1 α -Rev	5'-AAAGCTAGCATCGATGATATCCTCACGACACCTGAA ATGGAAGA-3'
MCS-sense	5'-ATCAGATCTCAATTGCTCGAGGCGGCCGCCAGCTGT CTAGACAT-3'
MCS-antisense	5'-CGATGTCTAGACAGCTGGCGGCCGCTCGAGCAATT GAGATCTGAT-3'
IRES-EGFP-Fwd	5'-AAATCTAGAGGCCGCTACGTAAATTCCG-3'
IRES-EGFP-Rev	5'-AAAATCGATGCTCGACTTACTTGTACAGCTCGTCCA TG -3'
IRES-Puro ^r -Fwd	5'-AAATCTAGACGGCCGCTACGTAAATTCCG-3'
IRES-Puro ^r -Rev	5'-AAAATCGATGCTCGATCAGGCACCGGGCTTGCGGGT -3'
3 \times FLAG-sense	5'-AAAAAGATCTACTACCATGGACTACAAAGACCATG ACGGTGATTATAAAGATCATGACAT-3'
3 \times FLAG-antisense	5'-TTTTCAATTGCTTGTTCATCGTCATCCTTGTAGTCGAT GTCATGATCTTTATAATCACCGT-3'
DPF1-Fwd	5'-GAATTCATGGGCGGCCTCAGCGCCCGCCCGA-3'
DPF1-Rev	5'-GTCGACGGTATCGATAAGCTTCTAGGTGAGGGTGAT GTAAGC-3'
DPF2-Fwd	5'-GAATTCATGGCGGCTGTGGTGGAGAAT-3'
DPF2-Rev	5'-GTCGACGGTATCGATAAGCTTTCAAGAGGAGTTCTG GTTCTGG-3'
DPF3a/b-Fwd	5'-GAATTCATGGCGACTGTCATTCACAAC-3'
DPF3a-Rev	5'-GTCGACGGTATCGATAAGCTTTTAGCAACTGCCCTT TTTATCTG-3'
DPF3b-Rev	5'-GTCGACGGTATCGATAAGCTTCTAGGCCTGGCAGCC AAA-3'
BRG1-Fwd	5'-CAATTGATGTCCACTCCAGACCCA-3'

BRG1-Rev	5'-TCTAGAGTCAGTCTTCTTCGCTGCCA-3'
Brm-Fwd	5'-GAATTCATGTCCACGCCACAGACCC-3'
Brm-Rev	5'-CTCGAGTCACTCATCATCCGTCCCAC-3'
BRG1(mutation)-Fwd	5'-ATATGATCGTCGACGAAGGTCACCGCATGAAGAAC- 3'
BRG1(mutation)-Rev	5'-ATTTCCATCTTATCTTGGCGAGGATGTGCTTGTCT-3'

Table 2. List of primer pairs used for qRT-PCR.

Gene	Forward primer	Reverse primer
<i>GAPDH</i>	CTCTGCTCCTCCTGTTTCGAC	TTAAAAGCAGCCCTGGTGAC
<i>Brm</i>	CAGAAGCAGAGCCGCATCA	GGCCTGAAGTCTGTATTCCCG
<i>BRG1</i>	AGATGTCTTCCGGGCCA	AGCTGGTTCTGGTTAAATGGG
<i>INI1</i>	GACGCCTTCACCTGGAACA	CGTCAGCGGGTTCAAATCCA
<i>BAF155</i>	TGACAGAGCAGACCAATCACA	AGAACTCAGGAAGAGCACGC
<i>BAF170</i>	ACGGCAAGAACAAGTCCAAGA	GGCAGGCGGTAGAGGTAAGA
<i>BAF60A</i>	TGGTAGAATGGCACAGGACCG	GGTAATCCAGCATCAGTAGGACA
<i>BAF60B</i>	AGGCGTACATGGATCTCTTGG	GCTGGGACTGAACGTATTGGA
<i>BAF60C</i>	TCATCAGCGTGGACCCTTCA	TTGGCCGTGGATAGGAGGAA
<i>BAF57</i>	GGTCACGGCATCCTCTGGTA	TCTCCACAACCTTTAGGTCAGG
<i>ARID1A</i>	CAGATGGGACACCCAAGACA	GTCCAGAGGTTTCTACCCAC
<i>ARID1B</i>	CGACTCTACGTCTGCGTCAA	CGTTTAGGTTGGTTGCCAGC
<i>BAF53A</i>	ACAGTGGAACGGAGGTTTAGC	GGGAACTCTTTCTCAAGGGCA
<i>BAF53B</i>	CGTCAAGTCTGAGCCAAACC	GCAGGAATGTTGTAAGTCTGCTCG
<i>DPF1</i>	CCGGAAGGGAGCTGGA	CAGGTAGGCGAGCACCAC
<i>DPF2</i>	CAGAGGAACAGGGAAGATGGC	ACTCCGGTCTGTGAGTCCAA
<i>DPF3a</i>	TCAGACAACACAGGAGCCAG	AACTGAGGCCATTCCCAAGG
<i>DPF3b</i>	AGCTACTCTTCTGCGATGACTG	TTCTCTTTGAGCAGTCCCAGC
<i>SS18</i>	GATGAACGGCCAGATGCCTG	TGATGATGGCACAGAATGGTTG
<i>CREST</i>	AACATGCAGTCCAACCCAGTCTC	CCTGCGCCGAGCTGTAGTG
<i>BRD9</i>	CTGCTCTACTCAGCCTACGG	GCATCCTTCACAAACTCCTGC
<i>BCL7A</i>	AGGCAAGGACGAGAAGTGTG	GCTGGAGTTGCTGCTGTTC
<i>BCL7B</i>	AAGTGGGTGACTGTGGGTGA	AGGCATCAGAAGGAAAGCCA
<i>BCL7C</i>	GGCCAAGAGAGAGATCCCG	CCTCAGCTTCCAGCAGTTC
<i>BCL11A</i>	CGCCGCAAGCAAGGCAA	CGTGGTCTGGTTCATCATCTGTAA
<i>BCL11B</i>	ATGGGGAGAGAAGGAGACTGAA	CGGCTGACGGTTACTTAGGAC
<i>POU3F2</i>	GCCCTCTTGTTCCCTCTCTAA	ACACATCATTACACCTGCTACC
<i>SOX2</i>	GAGGGGTGCAAAGAGGAGA	CGTGAGTGTGGATGGGATTG
<i>SALL2</i>	TCTTCCACCTTTACCACCCAC	AGATGAGGCGAGGCAATCAG
<i>OLIG2</i>	ACACAAATGGTAAACTCCTCCA	ACACGGCAGACGCTACAAA
<i>BMP4</i>	GGATCTTTACCGGCTTCAGTC	GGGATGTTCTCCAGATGTTCTTC
<i>p21</i>	GCAGACCAGCATGACAGATTTC	ATGTAGAGCGGGCCTTTGAG
<i>IL6</i>	AGTAACATGTGTGAAAGCAGCAA	AAACTCCAAAAGACCAGTGATGA

<i>IL8</i>	GGTGCAGTTTGGCCAAGGAG	TTCCTGGGGTCCAGACAGA
------------	----------------------	---------------------

Table 3. List of primary antibodies used in this study.

Application	Name	Host	Supplier	Catalog No.	Dilution
Western blotting	anti-SOX2	Rabbit	Abcam	ab92494	1/500
	anti-SALL2	Rabbit	Bethyl	A303-208A	1/2500
	anti-POU3F2	Goat	Santa Cruz	sc-6029	1/200
	anti-OLIG2	Rabbit	Millipore	AB9610	1/500
	anti- β -actin	Mouse	Santa Cruz	sc-47778	1/5000
	anti-BRG1	Rabbit	Santa Cruz	sc-10768	1/200
	anti-Brm	Rabbit	Abcam	ab15597	1/1000
	anti-BAF155	Goat	Santa Cruz	sc-9747	1/500
	anti-LSD1	Rabbit	Abcam	ab129195	1/1000
	anti-RCOR2	Rabbit	Santa Cruz	sc-102078	1/200
	anti-TLX	Mouse	Perseus Proteomics	PP-H6506-00	1/1000
	anti-HDAC2	Rabbit	Santa Cruz	sc-7899	1/200
Immunoprecipitation	normal rabbit IgG	Rabbit	Santa Cruz	sc-2027	2 μ g/sample
	normal mouse IgG	Mouse	Santa Cruz	sc-2025	2 μ g/sample
	anti-TLX	Mouse	Perseus Proteomics	PP-H6506-00	2 μ g/sample
	anti-LSD1	Rabbit	Abcam	ab17721	2 μ g/sample
	anti-RCOR2	Rabbit	Abcam	ab37113	2 μ g/sample
Immunofluorescence and proximity ligation assay	anti-BRG1	Mouse	Santa Cruz	sc-17796	1/50
	anti-BAF155	Rabbit	Abcam	ab72503	1/200
	anti-TLX	Rabbit	Santa Cruz	sc-292096	1/50
	anti-LSD1	Rabbit	Abcam	ab17721	1/200
	anti-LSD1	Mouse	Cell Signaling	#4218	1/100
	anti-FLAG	Mouse	Sigma-Aldrich	F1804	1/1000
	anti-RelA	Rabbit	Santa Cruz	sc-372	1/50
	anti-RelB	Rabbit	abcam	ab33907	1/100